

Charmless hadronic $B \rightarrow (f_1(1285), f_1(1420))P$ decays in the perturbative QCD approach

Xin Liu^{1a}, Zhen-Jun Xiao^{2b}, Jing-Wu Li^{1c}, and Zhi-Tian Zou^{3d}

¹ School of Physics and Electronic Engineering, Jiangsu Normal University, Xuzhou, Jiangsu 221116, People's Republic of China

² Department of Physics and Institute of Theoretical Physics,

Nanjing Normal University, Nanjing, Jiangsu 210023, People's Republic of China

³ Department of Physics, Yantai University, Yantai, Shandong 264005, People's Republic of China

(Dated: December 30, 2014)

We study 20 charmless hadronic $B \rightarrow f_1 P$ decays in the perturbative QCD(pQCD) formalism with B denoting B_u , B_d , and B_s mesons; P standing for the light pseudoscalar mesons; and f_1 representing axial-vector mesons $f_1(1285)$ and $f_1(1420)$ that result from a mixing of quark-flavor $f_{1q}[\frac{u\bar{u}+d\bar{d}}{\sqrt{2}}]$ and $f_{1s}[s\bar{s}]$ states with the angle ϕ_{f_1} . The estimations of CP -averaged branching ratios and CP asymmetries of the considered $B \rightarrow f_1 P$ decays, in which the $B_s \rightarrow f_1 P$ modes are investigated for the first time, are presented in the pQCD approach with $\phi_{f_1} \sim 24^\circ$ from recently measured $B_d/s \rightarrow J/\psi f_1(1285)$ decays. It is found that (a) the tree(penguin) dominant $B^+ \rightarrow f_1 \pi^+(K^+)$ decays with large branching ratios [$\mathcal{O}(10^{-6})$] and large direct CP violations (around 14% \sim 28% in magnitude) simultaneously are believed to be clearly measurable at the LHCb and Belle II experiments; (b) the $B_d \rightarrow f_1 K_S^0$ and $B_s \rightarrow f_1(\eta, \eta')$ decays with nearly pure penguin contributions and safely negligible tree pollution also have large decay rates in the order of $10^{-6} \sim 10^{-5}$, which can be confronted with the experimental measurements in the near future; (c) as the alternative channels, the $B^+ \rightarrow f_1(\pi^+, K^+)$ and $B_d \rightarrow f_1 K_S^0$ decays have the supplementary power in providing more effective constraints on the Cabibbo-Kobayashi-Maskawa weak phases α , γ , and β , correspondingly, which are explicitly analyzed through the large decay rates and the direct and mixing-induced CP asymmetries in the pQCD approach and are expected to be stringently examined by the measurements with high precision; (d) the weak annihilation amplitudes play important roles in the $B^+ \rightarrow f_1(1420)K^+$, $B_d \rightarrow f_1(1420)K_S^0$, $B_s \rightarrow f_1(1420)\eta'$ decays, and so on, which would offer more evidence, once they are confirmed by the experiments, to identify the soft-collinear effective theory and the pQCD approach on the evaluations of annihilation diagrams and to help further understand the annihilation mechanism in the heavy B meson decays; (e) combined with the future precise tests, the considered decays can provide more information to further understand the mixing angle ϕ_{f_1} and the nature of the f_1 mesons in depth after the confirmations on the reliability of the pQCD calculations in the present work.

PACS numbers: 13.25.Hw, 12.38.Bx, 14.40.Nd

I. INTRODUCTION

It is well known that nonleptonic weak decays of heavy B (specifically, B_u , B_d , B_s , and B_c) mesons can not only provide the important information to search for CP violation and further constrain the Cabibbo-Kobayashi-Maskawa (CKM) parameters in the standard model (SM), but also reveal the deviations from the SM, i.e., the signals of exotic new physics beyond the SM. Furthermore, comparison of theoretical predictions and experimental data for the physical observables may also help us understand the hadronic structure of the involved bound states deeply [1]. In contrast to the traditional $B \rightarrow PP$, PV , and VV decays, the alternative channels such as $B \rightarrow AP$ decays (A is the axial-vector meson) to be largely detected in experiments in the near future may give additional and complementary information on exclusive nonleptonic weak decays of heavy B mesons [2]; e.g., due to $V_{tb}^* V_{ts} = -V_{cb}^* V_{cs} [1 + \mathcal{O}(\lambda^2)]$, the $b \rightarrow sq\bar{q}$ penguin-dominated decays have the same CKM phase as the $b \rightarrow c\bar{c}s$ tree level decays [3]. Therefore, the $b \rightarrow sq\bar{q}$ mediated $B \rightarrow AP$ decays such as $B^0 \rightarrow a_1(1260)[b_1(1235)]K_S^0 \pi K_1(1270)[K_1(1400)]$, $f_1 K_S^0$ etc. can provide $\sin 2\beta$ measurements (β is the CKM weak phase) in the SM complementarily.

Very recently, the Large Hadron Collider beauty (LHCb) Collaboration reported the first measurements of $B_d/s \rightarrow J/\psi f_1(1285)$ decays [4], where the final state $f_1(1285)$ was observed for the first time in heavy B meson decays. In the conventional two quark structure, $f_1(1285)$ and its partner $f_1(1420)$ [5, 6] [hereafter, for the sake of simplicity, we will use f_1 to denote both $f_1(1285)$ and $f_1(1420)$ unless otherwise stated] are considered as the orbital excitation of the $q\bar{q}$ system, specifically, the light p -wave axial-vector flavorless mesons. In terms of the spectroscopic notation $(^{2S+1})L_J$ with $\mathbf{J} = \mathbf{L} + \mathbf{S}$, both f_1 mesons belong to 3P_1 nonet carrying the quantum number $J^{PC} = 1^{++}$ [3]. Similar to the $\eta - \eta'$ mixing in the pseudoscalar sector [3], these two f_1 mesons are believed to be a mixture resulting from the mixing between nonstrange $f_{1q} \equiv (u\bar{u} + d\bar{d})/\sqrt{2}$ and strange $f_{1s} \equiv s\bar{s}$ states in the popular quark-flavor basis with a single mixing angle ϕ_{f_1} . And for the mixing angle ϕ_{f_1} , there are several explorations that have been performed from theory and experiment sides. However, the value of ϕ_{f_1} is still in controversy presently (see Ref. [7] and references therein). It is necessary to point out that the mixing angle ϕ_{f_1} has important roles in

^a Electronic address: liuxin.physics@gmail.com

^b Electronic address: xiaozhenjun@njnu.edu.cn

^c Electronic address: lijw@jnsu.edu.cn

^d Electronic address: zouzt@ytu.edu.cn

investigating the properties of f_1 mesons themselves, but also of strange axial-vector K_1 mesons, i.e., $K_1(1270)$ and $K_1(1400)$, by constraining the mixing angle θ_{K_1} between two distinct types of axial-vector $K_{1A}({}^3P_1)$ and $K_{1B}({}^1P_1)$ states. The underlying reason is that when the $f_1(1285) - f_1(1420)$ mixing angle ϕ_{f_1} is determined from the mass relations related with the masses of K_{1A} and K_{1B} , it eventually depends on the mixing angle θ_{K_1} [8]. With the successful running of LHC and the forthcoming Belle II experiments, it is therefore expected that these first observations of $B_{d/s} \rightarrow J/\psi f_1(1285)$ decays will motivate the people to explore the mixing angle ϕ_{f_1} and the properties of both f_1 mesons in more relevant B meson decay processes at both experimental and theoretical aspects. Of course, in view of some of the axial-vector mesons such as $a_1(1260)$ and K_1 that have been seen in two-body hadronic D meson decays [3], it is also believed that the information on both f_1 mesons could be obtained from heavy c -quark decays in the near future.

In this work, we will therefore study 20 charmless hadronic $B \rightarrow f_1 P^1$ decays, in which B stands for B_u , B_d , and B_s , respectively, and P denotes the light pseudoscalar pion, kaon, and η and η' mesons. From the experimental point of view, up to now, only two penguin-dominated $B^+ \rightarrow f_1 K^+$ decays have been measured by the BABAR Collaboration in 2007 [13]. The preliminary upper limits on the decay rates have been placed at the 90% confidence level as [3]

$$Br(B^+ \rightarrow f_1(1285)K^+) < 2.0 \times 10^{-6}, \quad (1)$$

for $B^+ \rightarrow f_1(1285)K^+$ decay and

$$Br(B^+ \rightarrow f_1(1420)K^+) \cdot Br(f_1(1420) \rightarrow \bar{K}^* K) < 4.1 \times 10^{-6}, \quad (2)$$

$$Br(B^+ \rightarrow f_1(1420)K^+) \cdot Br(f_1(1420) \rightarrow \eta\pi\pi) < 2.9 \times 10^{-6}, \quad (3)$$

for $B^+ \rightarrow f_1(1420)K^+$ decay, respectively. However, due to the lack of the information on the decay rates of $f_1(1420) \rightarrow \bar{K}^* K$ and $f_1(1420) \rightarrow \eta\pi\pi$ decays, the upper limits of $Br(B^+ \rightarrow f_1(1420)K^+)$ cannot be extracted effectively. But, this status will be greatly improved in present and future experiments, notably at running LHCb and forthcoming Belle II. Also, other $B \rightarrow f_1 P$ decays are expected to be detected with good precision at the relevant experiments in the near future.

From the theoretical point of view, to our best knowledge, G. Calderón *et al.* have carried out the calculations of $B_{u,d} \rightarrow f_1 P$ decays in the framework of naive factorization with the form factors of $B \rightarrow f_1$ obtained in the improved Isgur-Scora-Grinstein-Wise quark model [2], while Cheng and Yang have studied the decay rates and direct CP asymmetries of $B_{u,d} \rightarrow f_1(\pi, K)$ modes within the framework of QCD factorization (QCDF) with the form factors evaluated in the QCD sum rule [14]. Note that the $B_s \rightarrow f_1 P$ decays have never been studied yet in any methods or approaches up to this date. And, it should be stressed that the predictions of the branching ratios for $B_{u,d} \rightarrow f_1 P$ decays in naive factorization are so crude that we cannot make effective comparison for relevant $B \rightarrow f_1 P$ modes. For $B^+ \rightarrow f_1 K^+$ decays for example, on one hand, the authors did not specify $f_1(1285)$ and $f_1(1420)$ [2], which then could not provide effectively the useful information on the mixing angle ϕ_{f_1} from these considered decays; on the other hand, as discussed in Ref. [14], the 3P_1 meson behaves analogously to the vector meson, it is then naively expected that $Br(B^+ \rightarrow f_1(1285)K^+) \sim Br(B^+ \rightarrow \omega K^+)$ and $Br(B^+ \rightarrow f_1(1420)K^+) \sim Br(B^+ \rightarrow \phi K^+)$ if $f_1(1285)$ and $f_1(1420)$ are significantly dominated by the f_{1q} and f_{1s} components, respectively. Furthermore, in principle, in view of the $f_1(1285) - f_1(1420)$ mixing, the branching ratios of $B^+ \rightarrow (f_1(1285), f_1(1420))K^+$ are generally a bit smaller than those of $B^+ \rightarrow (\omega, \phi)K^+$ ones correspondingly. However, the branching ratio of $B^+ \rightarrow f_1 K^+$ predicted in the naive factorization is around 3×10^{-5} , which is much larger than that of the corresponding VP modes, i.e., $B^+ \rightarrow \omega K^+$ and $B^+ \rightarrow \phi K^+$ [3]. As for the investigations of $B^+ \rightarrow f_1 K^+$ decays in the QCDF approach [14], the authors specified $f_1(1285)$ and $f_1(1420)$ and considered their mixing with two different sets of angles, $\theta_{3P_1} \sim 27.9^\circ$ and 53.2° , in the flavor singlet-octet basis. And the decay rates are barely consistent with the preliminary upper limits within very large errors. However, the pattern exhibited from the numerical results with $\theta_{3P_1} \sim 53.2^\circ$ is more favored by the available upper limits. As aforementioned, because of the similar behavior between the vector meson and 3P_1 axial-vector meson, the relation $Br(B^+ \rightarrow f_1(1285)K^+) < Br(B^+ \rightarrow f_1(1420)K^+)$ is expected to be highly preferred, as it should be.

In order to collect more information on the nature of both f_1 mesons and further understand the heavy flavor B physics, we will study the physical observables such as CP -averaged branching ratios and CP -violating asymmetries of 20 charmless hadronic $B \rightarrow f_1 P$ decays by employing the low energy effective Hamiltonian [15] and the pQCD approach [10–12] based on the k_T factorization theorem. Though some efforts have been made on the next-to-leading order pQCD formalism [16, 17], we here will still consider the perturbative evaluations at leading order, which are believed to be the dominant contributions perturbatively. As is well known, the pQCD approach is free of end-point singularity and the Sudakov formalism makes it more self-consistent by keeping the transverse momentum k_T of the quarks. More importantly, as the well-known advantage of the pQCD approach, we can explicitly calculate the weak annihilation types of diagrams without any parametrizations, apart from the traditional factorizable and nonfactorizable emission ones, though a different viewpoint on the evaluations and the magnitudes² of weak

¹ In the literature [9], two of us (X. Liu and Z.J. Xiao) have studied the $B_c \rightarrow f_1 P$ decays occurring only via the pure annihilation diagrams in the SM within the framework of the perturbative QCD(pQCD) factorization approach [10–12].

² As a matter of fact, the recent works [18, 19] in the framework of QCDF confirmed that there should exist complex annihilation contributions with large imaginary parts in $B_{u,d,s} \rightarrow \pi\pi, \pi K, KK$ decays by fits to the experimental data, which support the concept on the calculations of the annihilation diagrams in the pQCD approach [20] to some extent.

annihilation contributions has been proposed in the soft-collinear effective theory [21]. It is worth stressing that the pQCD predictions on the annihilation contributions in the heavy B meson decays have been tested at various aspects, e.g., see Refs. [10, 11, 22–26]. Typically, for example, the evaluations of the pure annihilation $B_d \rightarrow K^+ K^-$ and $B_s \rightarrow \pi^+ \pi^-$ decays in the pQCD approach [23–25] are in good consistency with the recent measurements by both CDF and LHCb Collaborations [27–29]. Therefore, the weak annihilation contributions to the considered $B \rightarrow f_1 P$ decays will be explicitly analyzed in this work, which are expected to be helpful to understand the annihilation mechanism in the heavy B meson decays.

The paper is organized as follows. In Sec. II, we present the formalism, hadron wave functions and perturbative calculations of the considered 20 $B \rightarrow f_1 P$ decays in the pQCD approach. The numerical results and the corresponding phenomenological analyses are addressed in Sec. III. Finally, Sec. IV contains the main conclusions and a short summary.

II. FORMALISM AND PERTURBATIVE CALCULATIONS

For the considered $B \rightarrow f_1 P$ decays, the related weak effective Hamiltonian H_{eff} [15] can be written as

$$H_{\text{eff}} = \frac{G_F}{\sqrt{2}} \left\{ V_{ub}^* V_{ud} [C_1(\mu) O_1^u(\mu) + C_2(\mu) O_2^u(\mu)] - V_{tb}^* V_{td} \left[\sum_{i=3}^{10} C_i(\mu) O_i(\mu) \right] \right\} + \text{H.c.}, \quad (4)$$

with D the light down-type quark d or s , the Fermi constant $G_F = 1.16639 \times 10^{-5} \text{GeV}^{-2}$, CKM matrix elements V , and Wilson coefficients $C_i(\mu)$ at the renormalization scale μ . The local four-quark operators $O_i (i = 1, \dots, 10)$ are written as

(1) current-current(tree) operators

$$O_1^u = (\bar{D}_\alpha u_\beta)_{V-A} (\bar{u}_\beta b_\alpha)_{V-A}, \quad O_2^u = (\bar{D}_\alpha u_\alpha)_{V-A} (\bar{u}_\beta b_\beta)_{V-A}; \quad (5)$$

(2) QCD penguin operators

$$\begin{aligned} O_3 &= (\bar{D}_\alpha b_\alpha)_{V-A} \sum_{q'} (\bar{q}'_\beta q'_\beta)_{V-A}, \quad O_4 = (\bar{D}_\alpha b_\beta)_{V-A} \sum_{q'} (\bar{q}'_\beta q'_\alpha)_{V-A}, \\ O_5 &= (\bar{D}_\alpha b_\alpha)_{V-A} \sum_{q'} (\bar{q}'_\beta q'_\beta)_{V+A}, \quad O_6 = (\bar{D}_\alpha b_\beta)_{V-A} \sum_{q'} (\bar{q}'_\beta q'_\alpha)_{V+A}; \end{aligned} \quad (6)$$

(3) electroweak penguin operators

$$\begin{aligned} O_7 &= \frac{3}{2} (\bar{D}_\alpha b_\alpha)_{V-A} \sum_{q'} e_{q'} (\bar{q}'_\beta q'_\beta)_{V+A}, \quad O_8 = \frac{3}{2} (\bar{D}_\alpha b_\beta)_{V-A} \sum_{q'} e_{q'} (\bar{q}'_\beta q'_\alpha)_{V+A}, \\ O_9 &= \frac{3}{2} (\bar{D}_\alpha b_\alpha)_{V-A} \sum_{q'} e_{q'} (\bar{q}'_\beta q'_\beta)_{V-A}, \quad O_{10} = \frac{3}{2} (\bar{D}_\alpha b_\beta)_{V-A} \sum_{q'} e_{q'} (\bar{q}'_\beta q'_\alpha)_{V-A}. \end{aligned} \quad (7)$$

with the color indices α, β (not to be confused with the CKM weak phases α and β) and the notations $(\bar{q}' q')_{V\pm A} = \bar{q}' \gamma_\mu (1 \pm \gamma_5) q'$. The index q' in the summation of the above operators runs through u, d, s, c , and b . The standard combinations a_i of the Wilson coefficients C_i are defined as follows:

$$a_1 = C_2 + \frac{C_1}{3}, \quad a_2 = C_1 + \frac{C_2}{3}, \quad a_i = C_i + C_{i\pm 1}/3, \quad i = 3 - 10. \quad (8)$$

where $C_2 \sim 1$ is the largest one among all Wilson coefficients and the upper (lower) sign applies, when i is odd (even). It is noted that, though the next-to-leading order Wilson coefficients have already been available [15], we will still adopt the leading order ones to keep the consistency, since the short distance contributions of the considered decays are calculated at leading order [$\mathcal{O}(\alpha_s)$] in the pQCD approach. This is also a consistent way to cancel the explicit μ dependence in the theoretical formulas. For the renormalization group evolution of the Wilson coefficients from higher scale to lower scale, the expressions are directly taken from Ref. [11].

Nowadays, the pQCD approach has been one of the popular factorization methods based on the QCD theory to evaluate the hadronic matrix elements in the heavy B meson decays. The unique point of the pQCD approach is that it keeps the transverse momentum k_T , which will act as an infrared regulator and smear the end-point singularity when the quark momentum fraction x approaches 0, of the valence quarks in the calculation of the hadronic matrix elements. Then, all the B meson transition form

factors, non-factorizable spectator and annihilation contributions are calculable in the framework of the k_T factorization. The decay amplitude of $B \rightarrow f_1 P$ decays in the pQCD approach can be conceptually written as

$$\mathcal{A}(B \rightarrow f_1 P) \sim \int d^4 k_1 d^4 k_2 d^4 k_3 \text{Tr} [C(t) \Phi_B(k_1) \Phi_{f_1}(k_2) \Phi_P(k_3) H(k_1, k_2, k_3, t)], \quad (9)$$

where k_i 's are the momenta of (light) quarks in the initial and final states, Tr represents the trace over Dirac and color indices, and $C(t)$ is the Wilson coefficient which results from the radiative corrections at short distance. In the above convolution, $C(t)$ includes the harder dynamics at larger scale than m_B scale and describes the evolution of local 4-Fermi operators from m_W (the W boson mass) down to $t \sim \mathcal{O}(\sqrt{\Lambda_{\text{QCD}} m_B})$ scale, where Λ_{QCD} is the hadronic scale. The Φ stands for the wave function describing hadronization of the quark and antiquark to the meson, which is independent of the specific processes and usually determined by employing nonperturbative QCD techniques such as lattice QCD (LQCD) or other well-measured processes. The function $H(k_1, k_2, k_3, t)$ describes the four-quark operator and the spectator quark connected by a hard gluon with the hard intermediate scale $\mathcal{O}(\sqrt{\Lambda_{\text{QCD}} m_B})$. Therefore, this hard part H can be calculated perturbatively.

Since the b quark is rather heavy, we thus work in the frame with the B meson at rest for simplicity, i.e., with the B meson momentum $P_1 = \frac{m_B}{\sqrt{2}}(1, 1, \mathbf{0}_T)$ in the light-cone coordinate. For the considered $B \rightarrow f_1 P$ decays, it is assumed that the f_1 and P mesons move in the plus and minus z direction carrying the momentum P_2 and P_3 , respectively. Then the momenta of the two final states can be written as

$$P_2 = \frac{m_B}{\sqrt{2}}(1, r_{f_1}^2, \mathbf{0}_T), \quad P_3 = \frac{m_B}{\sqrt{2}}(0, 1 - r_{f_1}^2, \mathbf{0}_T), \quad (10)$$

respectively, where $r_{f_1} = m_{f_1}/m_B$ and the masses of light pseudoscalar pion, kaon, and η and η' have been neglected. For the axial-vector meson f_1 , its longitudinal polarization vector $\epsilon_2^\mu = \frac{m_B}{\sqrt{2}m_{f_1}}(1, -r_{f_1}^2, \mathbf{0}_T)$. By choosing the quark momenta in B , f_1 and P mesons as k_1 , k_2 , and k_3 , respectively, and defining

$$k_1 = (x_1 P_1^+, 0, \mathbf{k}_{1T}), \quad k_2 = x_2 P_2 + (0, 0, \mathbf{k}_{2T}), \quad k_3 = x_3 P_3 + (0, 0, \mathbf{k}_{3T}). \quad (11)$$

then, the integration over k_1^- , k_2^- , and k_3^+ in Eq. (9) will give the more explicit form of decay amplitude in the pQCD approach,

$$\begin{aligned} \mathcal{A}(B \rightarrow f_1 P) \sim & \int dx_1 dx_2 dx_3 b_1 db_1 b_2 db_2 b_3 db_3 \\ & \cdot \text{Tr} \left[C(t) \Phi_B(x_1, b_1) \Phi_{f_1}(x_2, b_2) \Phi_P(x_3, b_3) H(x_i, b_i, t) S_t(x_i) e^{-S(t)} \right] \end{aligned} \quad (12)$$

where b_i is the conjugate space coordinate of k_{iT} , and t is the largest running scale in the hard kernel $H(x_i, b_i, t)$. The large logarithms $\ln(m_W/t)$ are included in the Wilson coefficients $C(t)$. Note that $S_t(x_i)$ and $e^{-S(t)}$ are the two important elements in the perturbative calculations with the pQCD approach. The former is a jet function from threshold resummation, which can strongly suppress the behavior in the small x region [30, 31]; while the latter is a Sudakov factor from k_T resummation, which can effectively suppress the soft dynamics in the small k_T region [32, 33]. These resummation effects therefore guarantee the removal of the end-point singularities. Thus it makes the perturbative calculation of the hard part H applicable at intermediate scale. We will calculate analytically the function $H(x_i, b_i, t)$ for the $B \rightarrow f_1 P$ decays at LO in the α_s expansion and give the convoluted amplitudes in the next section.

The heavy B meson is usually treated as a heavy-light system and its light-cone wave function can generally be defined as [10, 11, 34]

$$\Phi_B = \frac{i}{\sqrt{2N_c}} \{ (P^+ m_B) \gamma_5 \phi_B(x, k_T) \}_{\alpha\beta}; \quad (13)$$

in which α, β are the color indices; $P(m)$ is the momentum(mass) of the B meson; N_c is the color factor; and k_T is the intrinsic transverse momentum of the light quark in the B meson.

In Eq. (13), $\phi_B(x, k_T)$ is the B meson distribution amplitude, which satisfies the following normalization condition,

$$\int_0^1 dx \phi_B(x, b=0) = \frac{f_B}{2\sqrt{2N_c}}, \quad (14)$$

where b is the conjugate space coordinate of transverse momentum k_T and f_B is the decay constant of the B meson.

For the pseudoscalar P meson, the light-cone wave function can generally be defined as [35, 36]

$$\Phi_P(x) = \frac{i}{\sqrt{2N_c}} \gamma_5 \{ P \phi_P^A(x) + m_0^P \phi_P^P(x) + m_0^P (\not{p} - 1) \phi_P^T(x) \}_{\alpha\beta} \quad (15)$$

where ϕ_P^A and $\phi_P^{P,T}$ are the twist-2 and twist-3 distribution amplitudes, and m_0^P is the chiral enhancement factor of the meson, while x denotes the momentum fraction carried by quark in the meson and $n = (1, 0, \mathbf{0}_T)$ and $v = (0, 1, \mathbf{0}_T)$ are the dimensionless lightlike unit vectors.

The light-cone wave function of the axial-vector f_1 mesons has been given in the QCD sum rule as [37, 38]

$$\Phi_{f_1}^L = \frac{1}{\sqrt{2N_c}} \gamma_5 \left\{ m_{f_1} \not{\epsilon}_L \phi_{f_1}(x) + \not{\epsilon}_L P \phi_{f_1}^t(x) + m_{f_1} \phi_{f_1}^s(x) \right\}_{\alpha\beta}, \quad (16)$$

for longitudinal polarization with the polarization vector ϵ_L , satisfying $P \cdot \epsilon = 0$, where ϕ_{f_1} (not to be confused with the angle ϕ_{f_1} in the mixing of f_1 mesons) and $\phi_{f_1}^{s,t}$ are the twist-2 and twist-3 distribution amplitudes, respectively. All the explicit forms of the aforementioned hadronic distribution amplitudes in the considered $B \rightarrow f_1 P$ decays can be seen in the Appendix.

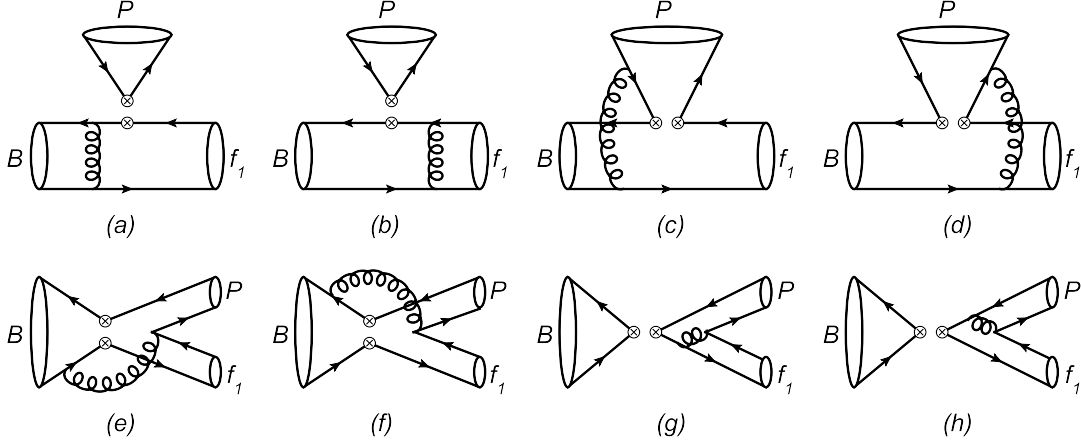


FIG. 1. Typical Feynman diagrams contributing to $B \rightarrow P f_1$ decays in the pQCD approach at leading order, in which P denotes the light pseudoscalar π , K , and η and η' mesons and f_1 stands for the axial-vector $f_1(1285)$ and $f_1(1420)$, respectively. When we exchange the positions of P and f_1 , the other eight diagrams contributing to the considered decays will be easily obtained.

Now we come to the analytically perturbative calculations of the factorization formulas for the $B \rightarrow f_1 P$ decays in the pQCD approach. From the effective Hamiltonian (4), there are eight types of diagrams contributing to the $B \rightarrow P f_1$ decays as illustrated in Fig. 1. For the factorizable emission(fe) diagrams, with Eq. (12), the analytic expressions of the decay amplitudes from different operators are given as follows:

- $(V - A)(V - A)$ operators:

$$F_{fe} = -8\pi C_F f_P m_B^2 \int_0^1 dx_1 dx_3 \int_0^\infty db_1 db_3 db_3 \phi_B(x_1, b_1) \{ [(1+x_3)\phi_{f_1}(x_3) + r_{f_1}(1-2x_3) \times (\phi_{f_1}^s(x_3) + \phi_{f_1}^t(x_3))] h_{fe}(x_1, x_3, b_1, b_3) E_{fe}(t_a) + 2 r_{f_1} \phi_{f_1}^s(x_3) h_{fe}(x_3, x_1, b_3, b_1) E_{fe}(t_b) \}, \quad (17)$$

- $(V - A)(V + A)$ operators:

$$F_{fe}^{P1} = -F_{fe}, \quad (18)$$

- $(S - P)(S + P)$ operators:

$$F_{fe}^{P2} = -16\pi C_F f_P m_B^2 r_0^P \int_0^1 dx_1 dx_3 \int_0^\infty db_1 db_3 db_3 \phi_B(x_1, b_1) \{ [\phi_{f_1}(x_3) + r_{f_1} [(2+x_3)\phi_{f_1}^s(x_3) - x_3\phi_{f_1}^t(x_3)]] h_{fe}(x_1, x_3, b_1, b_3) E_{fe}(t_a) + 2 r_{f_1} \phi_{f_1}^s(x_3) h_{fe}(x_3, x_1, b_3, b_1) E_{fe}(t_b) \}; \quad (19)$$

where $r_0^P = m_0^P/m_B$ and $C_F = 4/3$ is a color factor. The convolution functions E_i , the running hard scales t_i , and the hard functions h_i can be referred to in Ref. [39].

For the nonfactorizable emission(nfe) diagrams in Figs. 1(c) and 1(d), the corresponding decay amplitudes can be written as

- $(V - A)(V - A)$ operators:

$$M_{nfe} = -\frac{32}{\sqrt{6}}\pi C_F m_B^2 \int_0^1 dx_1 dx_2 dx_3 \int_0^\infty b_1 db_1 b_2 db_2 \phi_B(x_1, b_1) \phi_P^A(x_2) \\ \times \left\{ \left[(1-x_2) \phi_{f_1}(x_3) - r_{f_1} x_3 (\phi_{f_1}^s(x_3) - \phi_{f_1}^t(x_3)) \right] E_{nfe}(t_c) h_{nfe}^c(x_1, x_2, x_3, b_1, b_2) \right. \\ \left. - \left[(x_2+x_3) \phi_{f_1}(x_3) - r_{f_1} x_3 (\phi_{f_1}^s(x_3) + \phi_{f_1}^t(x_3)) \right] E_{nfe}(t_d) h_{nfe}^d(x_1, x_2, x_3, b_1, b_2) \right\}, \quad (20)$$

- $(V - A)(V + A)$ operators:

$$M_{nfe}^{P1} = -\frac{32}{\sqrt{6}}\pi C_F m_B^2 \int_0^1 dx_1 dx_2 dx_3 \int_0^\infty b_1 db_1 b_2 db_2 \phi_B(x_1, b_1) r_0^P \left\{ \left[(1-x_2) (\phi_P^P(x_2) + \phi_P^T(x_2)) \phi_{f_1}(x_3) - r_{f_1} \right. \right. \\ \times \left. \left. ((1-x_2-x_3) (\phi_P^P(x_2) \phi_{f_1}^t(x_3) - \phi_P^T(x_2) \phi_{f_1}^s(x_3)) - (1-x_2+x_3) (\phi_P^P(x_2) \phi_{f_1}^s(x_3) - \phi_P^T(x_2) \phi_{f_1}^t(x_3))) \right] \right. \\ \times E_{nfe}(t_c) h_{nfe}^c(x_1, x_2, x_3, b_1, b_2) - h_{nfe}^d(x_1, x_2, x_3, b_1, b_2) E_{nfe}(t_d) \left[x_2 (\phi_P^P(x_2) - \phi_P^T(x_2)) \phi_{f_1}(x_3) \right. \\ \left. \left. + r_{f_1} (x_2 (\phi_P^P(x_2) - \phi_P^T(x_2)) (\phi_{f_1}^s(x_3) - \phi_{f_1}^t(x_3)) + x_3 (\phi_P^P(x_2) + \phi_P^T(x_2)) (\phi_{f_1}^s(x_3) + \phi_{f_1}^t(x_3))) \right] \right\}, \quad (21)$$

- $(S - P)(S + P)$ operators:

$$M_{nfe}^{P2} = -\frac{32}{\sqrt{6}}\pi C_F m_B^2 \int_0^1 dx_1 dx_2 dx_3 \int_0^\infty b_1 db_1 b_2 db_2 \phi_B(x_1, b_1) \phi_P^A(x_2) \\ \times \left\{ \left[(x_2-x_3-1) \phi_{f_1}(x_3) + r_{f_1} x_3 (\phi_{f_1}^s(x_3) + \phi_{f_1}^t(x_3)) \right] E_{nfe}(t_c) h_{nfe}^c(x_1, x_2, x_3, b_1, b_2) \right. \\ \left. + \left[x_2 \phi_{f_1}(x_3) - r_{f_1} x_3 (\phi_{f_1}^s(x_3) - \phi_{f_1}^t(x_3)) \right] h_{nfe}^d(x_1, x_2, x_3, b_1, b_2) E_{nfe}(t_d) \right\}; \quad (22)$$

The Feynman diagrams shown in Figs. 1(e) and 1(f) are the nonfactorizable annihilation(*nfa*) ones, whose contributions are

- $(V - A)(V - A)$ operators:

$$M_{nfa} = -\frac{32}{\sqrt{6}}\pi C_F m_B^2 \int_0^1 dx_1 dx_2 dx_3 \int_0^\infty b_1 db_1 b_2 db_2 \phi_B(x_1, b_1) \left\{ \left[(1-x_3) \phi_P^A(x_2) \phi_{f_1}(x_3) + r_0^P r_{f_1} (\phi_P^P(x_2) \right. \right. \\ \times \left. \left. [(1+x_2-x_3) \phi_{f_1}^s(x_3) - (1-x_2-x_3) \phi_{f_1}^t(x_3)] + \phi_P^T(x_2) [(1-x_2-x_3) \phi_{f_1}^s(x_3) - (1+x_2-x_3) \right. \right. \\ \times \left. \left. \phi_{f_1}^t(x_3)] \right] \right] E_{nfa}(t_e) h_{nfa}^e(x_1, x_2, x_3, b_1, b_2) - E_{nfa}(t_f) h_{nfa}^f(x_1, x_2, x_3, b_1, b_2) \left[x_2 \phi_P^A(x_2) \phi_{f_1}(x_3) \right. \\ \left. + r_0^P r_{f_1} (\phi_P^P(x_2) [(x_2-x_3+3) \phi_{f_1}^s(x_3) + (1-x_2-x_3) \phi_{f_1}^t(x_3)] + \phi_P^T(x_2) [(x_2+x_3-1) \phi_{f_1}^s(x_3) \right. \\ \left. \left. + (1-x_2+x_3) \phi_{f_1}^t(x_3)] \right] \right\}, \quad (23)$$

- $(V - A)(V + A)$ operators:

$$M_{nfa}^{P1} = -\frac{32}{\sqrt{6}}\pi C_F m_B^2 \int_0^1 dx_1 dx_2 dx_3 \int_0^\infty b_1 db_1 b_2 db_2 \phi_B(x_1, b_1) \left\{ \left[r_0^P x_2 \phi_{f_1}(x_3) (\phi_P^P(x_2) + \phi_P^T(x_2)) \right. \right. \\ \left. \left. - r_{f_1} (1-x_3) \phi_P^A(x_2) (\phi_{f_1}^s(x_3) - \phi_{f_1}^t(x_3)) \right] E_{nfa}(t_e) h_{nfa}^e(x_1, x_2, x_3, b_1, b_2) + h_{nfa}^f(x_1, x_2, x_3, b_1, b_2) \right. \\ \left. \times \left[r_0^P (2-x_2) (\phi_P^P(x_2) + \phi_P^T(x_2)) \phi_{f_1}(x_3) - r_{f_1} (1+x_3) \phi_P^A(x_2) (\phi_{f_1}^s(x_3) - \phi_{f_1}^t(x_3)) \right] E_{nfa}(t_f) \right\}, \quad (24)$$

- $(S - P)(S + P)$ operators:

$$M_{nfa}^{P2} = \frac{32}{\sqrt{6}}\pi C_F m_B^2 \int_0^1 dx_1 dx_2 dx_3 \int_0^\infty b_1 db_1 b_2 db_2 \phi_B(x_1, b_1) \left\{ \left[(1-x_3) \phi_P^A(x_2) \phi_{f_1}(x_3) + r_0^P r_{f_1} (\phi_P^P(x_2) \right. \right. \\ \times \left. \left. [(x_2-x_3+3) \phi_{f_1}^s(x_3) - (1-x_2-x_3) \phi_{f_1}^t(x_3)] + \phi_P^T(x_2) [(1-x_2-x_3) \phi_{f_1}^s(x_3) + (1-x_2+x_3) \right. \right. \\ \times \left. \left. \phi_{f_1}^t(x_3)] \right] \right] E_{nfa}(t_f) h_{nfa}^f(x_1, x_2, x_3, b_1, b_2) - E_{nfa}(t_e) h_{nfa}^e(x_1, x_2, x_3, b_1, b_2) \left[x_2 \phi_P^A(x_2) \phi_{f_1}(x_3) \right. \\ \left. \left. + r_0^P r_{f_1} (x_2 (\phi_P^P(x_2) + \phi_P^T(x_2)) (\phi_{f_1}^s(x_3) - \phi_{f_1}^t(x_3)) + (1-x_3) (\phi_P^P(x_2) - \phi_P^T(x_2)) (\phi_{f_1}^s(x_3) + \phi_{f_1}^t(x_3))) \right] \right\} \quad (25)$$

For the last two diagrams in Fig. 1, i.e., the factorizable annihilation(*fa*) diagrams 1(g) and 1(h), we have

- $(V - A)(V - A)$ operators:

$$F_{fa} = -8\pi C_F m_B^2 \int_0^1 dx_2 dx_3 \int_0^\infty b_2 db_2 b_3 db_3 \{ [x_2 \phi_P^A(x_2) \phi_{f_1}(x_3) - 2r_0^P r_{f_1} ((x_2 + 1)\phi_P^P(x_2) + (x_2 - 1)\phi_P^T(x_2)) \times \phi_{f_1}^s(x_3)] h_{fa}(x_2, 1 - x_3, b_2, b_3) E_{fa}(t_g) - [(1 - x_3)\phi_P^A(x_2) \phi_{f_1}(x_3) - 2r_0^P r_{f_1} \phi_P^P(x_2) ((x_3 - 2)\phi_{f_1}^s(x_3) - x_3 \phi_{f_1}^t(x_3))] E_{fa}(t_h) h_{fa}(1 - x_3, x_2, b_3, b_2) \} , \quad (26)$$

- $(V - A)(V + A)$ operators:

$$F_{fa}^{P1} = F_{fa} , \quad (27)$$

- $(S - P)(S + P)$ operators:

$$F_{fa}^{P2} = -16\pi C_F m_B^2 \int_0^1 dx_2 dx_3 \int_0^\infty b_2 db_2 b_3 db_3 \{ [2r_{f_1} \phi_P^A(x_2) \phi_{f_1}^s(x_3) + r_0^P x_2 (\phi_P^P(x_2) - \phi_P^T(x_2)) \phi_{f_1}(x_3)] \times E_{fa}(t_g) h_{fa}(x_2, 1 - x_3, b_2, b_3) + [r_{f_1} (1 - x_3) \phi_P^A(x_2) (\phi_{f_1}^s(x_3) + \phi_{f_1}^t(x_3)) + 2r_0^P \phi_P^P(x_2) \phi_{f_1}(x_3)] \times E_{fa}(t_h) h_{fa}(1 - x_3, x_2, b_3, b_2) \} . \quad (28)$$

When we exchange P and f_1 in Fig. 1, we can obtain the new eight diagrams contributing to the considered $B \rightarrow f_1 P$ decays. The corresponding factorization formulas can be easily obtained with the simple replacements in Eqs. (17)-(28) as follows,

$$f_P \longleftrightarrow f_{f_1} , \quad \phi_P^A \longleftrightarrow \phi_{f_1} , \quad \phi_P^P \longleftrightarrow \phi_{f_1}^s , \quad \phi_P^T \longleftrightarrow \phi_{f_1}^t , \quad r_0^P \longleftrightarrow r_{f_1} , \quad (29)$$

where F' and M' will be used to denote the Feynman amplitudes from these new diagrams. Note that, due to $\langle f_1 | S \pm P | 0 \rangle = 0$, the factorizable emission amplitude F_{fe}^{P2} is therefore absent naturally.

Before we write down the total decay amplitudes for the $B \rightarrow f_1 P$ modes, it is essential to give a brief discussion about the $\eta - \eta'$ mixing and $f_1(1285) - f_1(1420)$ mixing, respectively. The $\eta - \eta'$ mixing has been discussed in different bases: quark-flavor basis [40] and octet-singlet basis [41], and the related parameters have been effectively constrained from various experiments and theories (for a recently detailed overview, see [42] and references therein). In the present work, we adopt the quark-flavor basis with the definitions [40] $\eta_q = (u\bar{u} + d\bar{d})/\sqrt{2}$ and $\eta_s = s\bar{s}$. Then the physical states η and η' can be described as the mixtures of two quark-flavor η_q and η_s states with a single mixing angle ϕ ,

$$\begin{pmatrix} \eta \\ \eta' \end{pmatrix} = U(\phi) \begin{pmatrix} \eta_q \\ \eta_s \end{pmatrix} = \begin{pmatrix} \cos \phi & -\sin \phi \\ \sin \phi & \cos \phi \end{pmatrix} \begin{pmatrix} \eta_q \\ \eta_s \end{pmatrix}. \quad (30)$$

It is assumed that the η_q and η_s states have the same light-cone distribution amplitudes as that of the pion but with different decay constants f_{η_q} and f_{η_s} and different chiral enhancement factors $m_0^{\eta_q}$ and $m_0^{\eta_s}$. The f_{η_q} , f_{η_s} and ϕ in the quark-flavor basis have been extracted from various related experiments [40, 41]:

$$f_{\eta_q} = (1.07 \pm 0.02) f_\pi, \quad f_{\eta_s} = (1.34 \pm 0.06) f_\pi, \quad \phi = 39.3^\circ \pm 1.0^\circ. \quad (31)$$

And the chiral enhancement factors are chosen as

$$m_0^{\eta_q} = \frac{1}{2m_q} [m_\eta^2 \cos^2 \phi + m_{\eta'}^2 \sin^2 \phi - \frac{\sqrt{2} f_{\eta_s}}{f_{\eta_q}} (m_{\eta'}^2 - m_\eta^2) \cos \phi \sin \phi], \quad (32)$$

$$m_0^{\eta_s} = \frac{1}{2m_s} [m_{\eta'}^2 \cos^2 \phi + m_\eta^2 \sin^2 \phi - \frac{f_{\eta_q}}{\sqrt{2} f_{\eta_s}} (m_{\eta'}^2 - m_\eta^2) \cos \phi \sin \phi]. \quad (33)$$

with no isospin violation, i.e., the mass $m_q = m_u = m_d$. It is worth mentioning that the effects of the possible gluonic component of the η' meson will not be considered here, since it is small in size [39, 43–45].

Likewise, by considering both f_1 mesons as the mixed quark flavor states, then this $f_1(1285) - f_1(1420)$ mixing can also be described as a 2×2 rotation matrix with a single angle ϕ_{f_1} in the quark-flavor basis [4], although there are also two mixing schemes for the $f_1(1285) - f_1(1420)$ mixing system [5, 8, 14, 37, 46, 47]:

$$\begin{pmatrix} f_1(1285) \\ f_1(1420) \end{pmatrix} = \begin{pmatrix} \cos \phi_{f_1} & -\sin \phi_{f_1} \\ \sin \phi_{f_1} & \cos \phi_{f_1} \end{pmatrix} \begin{pmatrix} f_{1q} \\ f_{1s} \end{pmatrix}. \quad (34)$$

As discussed in Ref. [7], since the axial-vector mesons have similar behavior to that of the vector ones, and the vector mesons ρ and ω have the same distribution amplitudes, except for the different decay constants f_ρ and f_ω , we therefore assume that

the f_{1q} distribution amplitude is the same one as $a_1(1260)$ with decay constant $f_{f_{1q}} = 0.193^{+0.043}_{-0.038}$ GeV [48]. For the f_{1s} state, for the sake of simplicity, we adopt the same distribution amplitude as flavor singlet f_1 state [not to be confused with the abbreviation f_1 of $f_1(1285)$ and $f_1(1420)$ mesons] [7], but with decay constant $f_{f_{1s}} = 0.230 \pm 0.009$ GeV [48]. For the masses of two f_{1q} and f_{1s} states, we adopt $m_{f_{1q}} \sim m_{f_1(1285)}$ and $m_{f_{1s}} \sim m_{f_1(1420)}$ for convenience. Another more important factor is the value of the mixing angle ϕ_{f_1} , which is less constrained from the experiments currently. Up to now, we just have some limited information on ϕ_{f_1} still in controversy at the theoretical and experimental aspects: (1) $(15^{+5}_{-10})^\circ$ provided by the Mark-II detector at SLAC from the ratio of $\frac{\Gamma(f_1(1285) \rightarrow \gamma\gamma^*)}{\Gamma(f_1(1420) \rightarrow \gamma\gamma^*)}$ [49]; (2) $(15.8^{+4.5}_{-4.6})^\circ$ extracted from the radiative $f_1(1285) \rightarrow \phi\gamma$ and $\rho\gamma$ decays [46] phenomenologically; (3) $(27 \pm 2)^\circ$ from the updated LQCD calculations [50]; and (4) $(24.0^{+3.2}_{-2.7})^\circ$ measured first from the $B_{d/s} \rightarrow J/\psi f_1(1285)$ decays by the LHCb Collaboration [4] very recently. In view of the good consistency for the values of ϕ_{f_1} between the latest measurements in B meson decays and the latest calculations in LQCD, we will adopt $\phi_{f_1} = 24^\circ$ as input in the numerical evaluations.

Thus, by combining various contributions from different diagrams, the total decay amplitudes for 20 charmless hadronic $B \rightarrow f_1 P$ decays in the pQCD approach can be written as

1. $B^+ \rightarrow f_1(1285)(\pi^+, K^+)$ decays

$$\begin{aligned} \mathcal{A}(B^+ \rightarrow f_1(1285)\pi^+) = & \left\{ [a_1](f_\pi F_{fe} + f_B F_{fa} + f_B F'_{fa}) + [a_2]f_{f_{1q}} F'_{fe} + [C_1](M_{nfe} + M_{nfa} + M'_{nfa}) \right. \\ & + [C_2]M'_{nfe} \left. \right\} \lambda_u^d \zeta_{f_{1q}} - \lambda_t^d \zeta_{f_{1q}} \left\{ [a_4 + a_{10}](f_\pi F_{fe} + f_B F_{fa} + f_B F'_{fa}) + [a_6 + a_8] \right. \\ & \cdot (f_\pi F_{fe}^{P_2} + f_B F_{fa}^{P_2} + f_B F'_{fa}^{P_2}) + [C_3 + C_9](M_{nfe} + M_{nfa} + M'_{nfa}) + [C_5 + C_7] \\ & \cdot (M_{nfe}^{P_1} + M_{nfa}^{P_1} + M'_{nfa}^{P_1}) + [2a_3 + a_4 - 2a_5 - \frac{1}{2}(a_7 - a_9 + a_{10})]f_{f_{1q}} F'_{fe} + [C_3 \\ & + 2C_4 - \frac{1}{2}(C_9 - C_{10})]M'_{nfe} + [C_5 - \frac{1}{2}C_7]M_{nfe}^{P_1} + [2C_6 + \frac{1}{2}C_8]M_{nfe}^{P_2} \left. \right\} - \lambda_t^d \zeta_{f_{1s}} \\ & \cdot \left\{ [a_3 - a_5 + \frac{1}{2}(a_7 - a_9)]f_{f_{1s}} F'_{fe} + [C_4 - \frac{1}{2}C_{10}]M'_{nfe} + [C_6 - \frac{1}{2}C_8]M_{nfe}^{P_2} \right\}; \quad (35) \end{aligned}$$

$$\begin{aligned} \mathcal{A}(B^+ \rightarrow f_1(1285)K^+) = & \lambda_u^s \left\{ [a_1] \left((f_K F_{fe} + f_B F_{fa})\zeta_{f_{1q}} + f_B F'_{fa}\zeta_{f_{1s}} \right) + [a_2]f_{f_{1q}} F'_{fe}\zeta_{f_{1q}} + [C_1] \left(M'_{nfa}\zeta_{f_{1s}} \right. \right. \\ & + (M_{nfe} + M_{nfa})\zeta_{f_{1q}} \left. \right) + [C_2]M'_{nfe}\zeta_{f_{1q}} \left. \right\} - \lambda_t^s \left\{ [a_4 + a_{10}] \left((f_K F_{fe} + f_B F_{fa})\zeta_{f_{1q}} \right. \right. \\ & + f_B F'_{fa}\zeta_{f_{1s}} \left. \right) + [a_6 + a_8] \left((f_K F_{fe}^{P_2} + f_B F_{fa}^{P_2})\zeta_{f_{1q}} + f_B F'_{fa}^{P_2}\zeta_{f_{1s}} \right) + [C_3 + C_9] \\ & \cdot \left(M'_{nfa}\zeta_{f_{1s}} + (M_{nfe} + M_{nfa})\zeta_{f_{1q}} \right) + [C_5 + C_7] \left((M_{nfe}^{P_1} + M_{nfa}^{P_1})\zeta_{f_{1q}} + M'_{nfa}^{P_1}\zeta_{f_{1s}} \right) \\ & + \left([2a_3 - 2a_5 - \frac{1}{2}(a_7 - a_9)]f_{f_{1q}} F'_{fe} + [2C_4 + \frac{1}{2}C_{10}]M'_{nfe} + [2C_6 + \frac{1}{2}C_8]M_{nfe}^{P_2} \right) \zeta_{f_{1q}} \\ & + \left([a_3 + a_4 - a_5 + \frac{1}{2}(a_7 - a_9 - a_{10})]f_{f_{1s}} F'_{fe} + [C_3 + C_4 - \frac{1}{2}(C_9 + C_{10})]M'_{nfe} \right. \\ & + [C_5 - \frac{1}{2}C_7]M_{nfe}^{P_1} + [C_6 - \frac{1}{2}C_8]M_{nfe}^{P_2} \left. \right) \zeta_{f_{1s}} \left. \right\}; \quad (36) \end{aligned}$$

2. $B_d^0 \rightarrow f_1(1285)(\pi^0, K^0, \eta, \eta')$ decays

$$\begin{aligned}
\sqrt{2}\mathcal{A}(B_d^0 \rightarrow f_1(1285)\pi^0) = & \left\{ [a_2](f_\pi F_{fe} + f_B F_{fa} + f_B F'_{fa} - f_{f_{1q}} F'_{fe}) + [C_2](M_{nfe} + M_{nfa} + M'_{nfa} - M'_{nfe}) \right\} \\
& \cdot \lambda_u^d \zeta_{f_{1q}} - \lambda_t^d \zeta_{f_{1q}} \left\{ [-a_4 - \frac{1}{2}(3a_7 - 3a_9 - a_{10})] f_\pi F_{fe} + [-a_4 + \frac{1}{2}(3a_7 + 3a_9 + a_{10})] \right. \\
& \cdot (f_B F_{fa} + f_B F'_{fa}) - [2a_3 + a_4 - 2a_5 - \frac{1}{2}(a_7 - a_9 + a_{10})] f_{f_{1q}} F'_{fe} - [a_6 - \frac{1}{2}a_8] (f_\pi \\
& \cdot F_{fe}^{P_2} + f_B F_{fa}^{P_2} + f_B F'_{fa}^{P_2}) + [-C_3 + \frac{1}{2}(C_9 + 3C_{10})] (M_{nfe} + M_{nfa} + M'_{nfa}) + [\frac{3}{2}C_8] \\
& \cdot (M_{nfe}^{P_2} + M_{nfa}^{P_2} + M'_{nfa}^{P_2}) - [C_5 - \frac{1}{2}C_7] (M_{nfe}^{P_1} + M_{nfa}^{P_1} + M'_{nfa}^{P_1} + M'_{nfe}^{P_1}) - [C_3 + 2C_4 \\
& - \frac{1}{2}(C_9 - C_{10})] M'_{nfe} - [2C_6 + \frac{1}{2}C_8] M_{nfe}^{P_2} \left. \right\} - \lambda_t^d \left\{ -[a_3 - a_5 + \frac{1}{2}(a_7 - a_9)] f_{f_{1s}} F'_{fe} \right. \\
& \left. - [C_4 - \frac{1}{2}C_{10}] M'_{nfe} - [C_6 - \frac{1}{2}C_8] M_{nfe}^{P_2} \right\} \zeta_{f_{1s}}; \tag{37}
\end{aligned}$$

$$\begin{aligned}
\mathcal{A}(B_d^0 \rightarrow f_1(1285)K^0) = & \lambda_u^s \left\{ [a_2] f_{f_{1q}} F'_{fe} + [C_2] M'_{nfe} \right\} \zeta_{f_{1q}} - \lambda_t^s \left\{ [a_4 - \frac{1}{2}a_{10}] \left((f_K F_{fe} + f_B F_{fa}) \zeta_{f_{1q}} + \zeta_{f_{1s}} \right. \right. \\
& \cdot f_B F'_{fa} \left. \right) + [a_6 - \frac{1}{2}a_8] \left((f_K F_{fe}^{P_2} + f_B F_{fa}^{P_2}) \zeta_{f_{1q}} + f_B F_{fa}^{P_2} \zeta_{f_{1s}} \right) + [C_3 - \frac{1}{2}C_9] \\
& \cdot \left((M_{nfe} + M_{nfa}) \zeta_{f_{1q}} + M'_{nfa} \zeta_{f_{1s}} \right) + [C_5 - \frac{1}{2}C_7] \left((M_{nfe}^{P_1} + M_{nfa}^{P_1}) \zeta_{f_{1q}} + M'_{nfa}^{P_1} \zeta_{f_{1s}} \right) \\
& + \left([2a_3 - 2a_5 - \frac{1}{2}(a_7 - a_9)] f_{f_{1q}} F'_{fe} + [2C_4 + \frac{1}{2}C_{10}] M'_{nfe} + [2C_6 + \frac{1}{2}C_8] M_{nfe}^{P_2} \right) \zeta_{f_{1q}} \\
& + \left([a_3 + a_4 - a_5 + \frac{1}{2}(a_7 - a_9 - a_{10})] f_{f_{1s}} F'_{fe} + [C_3 + C_4 - \frac{1}{2}(C_9 + C_{10})] M'_{nfe} \right. \\
& \left. + [C_5 - \frac{1}{2}C_7] M_{nfe}^{P_1} + [C_6 - \frac{1}{2}C_8] M_{nfe}^{P_2} \right) \zeta_{f_{1s}} \left. \right\}; \tag{38}
\end{aligned}$$

$$\begin{aligned}
\mathcal{A}(B_d^0 \rightarrow f_1(1285)\eta) = & \lambda_u^d \left\{ [a_2] (f_{\eta_q} F_{fe} + f_B F_{fa} + f_B F'_{fa} + f_{f_{1q}} F'_{fe}) + [C_2] (M_{nfe} + M_{nfa} + M'_{nfa} + M'_{nfe}) \right\} \\
& \cdot \zeta_{f_{1q}} \cdot \zeta_{\eta_q} - \lambda_t^d \left\{ [2a_3 + a_4 - 2a_5 - \frac{1}{2}(a_7 - a_9 + a_{10})] (f_{\eta_q} F_{fe} + f_{f_{1q}} F'_{fe}) + [2a_3 + a_4 \right. \\
& + 2a_5 + \frac{1}{2}(a_7 + a_9 - a_{10})] (f_B F_{fa} + f_B F'_{fa}) + [a_6 - \frac{1}{2}a_8] (f_{\eta_q} F_{fe}^{P_2} + f_B F_{fa}^{P_2} + f_B F_{fa}^{P_2}) \\
& + [C_3 + 2C_4 - \frac{1}{2}(C_9 - C_{10})] (M_{nfe} + M'_{nfe} + M_{nfa} + M'_{nfa}) + [C_5 - \frac{1}{2}C_7] (M_{nfe}^{P_1} \\
& + M_{nfa}^{P_1} + M'_{nfa}^{P_1} + M'_{nfe}^{P_1}) + [2C_6 + \frac{1}{2}C_8] (M_{nfe}^{P_2} + M'_{nfe}^{P_2} + M_{nfa}^{P_2} + M'_{nfa}^{P_2}) \left. \right\} \cdot \zeta_{f_{1q}} \cdot \zeta_{\eta_q} \\
& - \lambda_t^d \left\{ [a_3 - a_5 + \frac{1}{2}(a_7 - a_9)] \left(f_{\eta_s} F_{fe} \zeta_{\eta_s} \cdot \zeta_{f_{1q}} + f_{f_{1s}} F'_{fe} \cdot \zeta_{f_{1s}} \cdot \zeta_{\eta_q} \right) + [a_3 + a_5 - \frac{1}{2} \right. \\
& \cdot (a_7 + a_9)] (f_B F_{fa} + f_B F'_{fa}) \zeta_{\eta_s} \cdot \zeta_{f_{1s}} + [C_4 - \frac{1}{2}C_{10}] \left(M_{nfe} \zeta_{\eta_s} \cdot \zeta_{f_{1q}} + M'_{nfe} \zeta_{f_{1s}} \cdot \zeta_{\eta_q} \right. \\
& + (M_{nfa} + M'_{nfa}) \zeta_{\eta_s} \zeta_{f_{1s}} \left. \right) + [C_6 - \frac{1}{2}C_8] \left(M_{nfe}^{P_2} \zeta_{\eta_s} \cdot \zeta_{f_{1q}} + M'_{nfe}^{P_2} \zeta_{f_{1s}} \cdot \zeta_{\eta_q} + (M_{nfa}^{P_2} \right. \\
& \left. + M'_{nfa}^{P_2}) \zeta_{\eta_s} \cdot \zeta_{f_{1s}} \right) \left. \right\}; \tag{39}
\end{aligned}$$

$$\begin{aligned}
\mathcal{A}(B_d^0 \rightarrow f_1(1285)\eta') = & \left\{ [a_2](f_{\eta_q}F_{fe} + f_B F_{fa} + f_B F'_{fa} + f_{f_{1q}}F'_{fe}) + [C_2](M_{nfe} + M_{nfa} + M'_{nfa} + M'_{nfe}) \right\} \\
& \cdot \lambda_u^d \cdot \zeta_{f_{1q}} \cdot \zeta'_{\eta_q} - \lambda_t^d \left\{ [2a_3 + a_4 - 2a_5 - \frac{1}{2}(a_7 - a_9 + a_{10})](f_{\eta_q}F_{fe} + f_{f_{1q}}F'_{fe}) + [2a_3 \right. \\
& + a_4 + 2a_5 + \frac{1}{2}(a_7 + a_9 - a_{10})](f_B F_{fa} + f_B F'_{fa}) + [a_6 - \frac{1}{2}a_8](f_{\eta_q}F_{fe}^{P_2} + f_B F_{fa}^{P_2} \\
& + f_B F_{fa}'^{P_2}) + [C_3 + 2C_4 - \frac{1}{2}(C_9 - C_{10})](M_{nfe} + M'_{nfe} + M_{nfa} + M'_{nfa}) + [C_5 - \frac{1}{2}C_7] \\
& \cdot (M_{nfe}^{P_1} + M_{nfa}^{P_1} + M_{nfa}'^{P_1} + M_{nfe}'^{P_1}) + [2C_6 + \frac{1}{2}C_8](M_{nfe}^{P_2} + M_{nfe}'^{P_2} + M_{nfa}^{P_2} + M_{nfa}'^{P_2}) \left. \right\} \\
& \cdot \zeta_{f_{1q}} \cdot \zeta'_{\eta_q} - \lambda_t^d \left\{ [a_3 - a_5 + \frac{1}{2}(a_7 - a_9)] \left(f_{\eta_s} F_{fe} \zeta'_{\eta_s} \cdot \zeta_{f_{1q}} + f_{f_{1s}} F'_{fe} \cdot \zeta_{f_{1s}} \cdot \zeta'_{\eta_q} \right) + [a_3 \right. \\
& + a_5 - \frac{1}{2}(a_7 + a_9)](f_B F_{fa} + f_B F'_{fa}) \zeta'_{\eta_s} \cdot \zeta_{f_{1s}} + [C_4 - \frac{1}{2}C_{10}] \left(M_{nfe} \zeta'_{\eta_s} \cdot \zeta_{f_{1q}} + M'_{nfe} \right. \\
& \cdot \zeta_{f_{1s}} \cdot \zeta'_{\eta_q} + (M_{nfa} + M'_{nfa}) \zeta'_{\eta_s} \cdot \zeta_{f_{1s}} \left. \right) + [C_6 - \frac{1}{2}C_8] \left(M_{nfe}^{P_2} \zeta'_{\eta_s} \cdot \zeta_{f_{1q}} + M_{nfe}'^{P_2} \zeta_{f_{1s}} \cdot \zeta'_{\eta_q} \right. \\
& \left. \left. + (M_{nfa}^{P_2} + M_{nfa}'^{P_2}) \zeta'_{\eta_s} \cdot \zeta_{f_{1s}} \right) \right\}; \tag{40}
\end{aligned}$$

3. $B_s^0 \rightarrow f_1(1285)(\pi^0, \bar{K}^0, \eta, \eta')$ decays

$$\begin{aligned}
\sqrt{2}\mathcal{A}(B_s^0 \rightarrow f_1(1285)\pi^0) = & \left\{ [a_2] \left(f_{\pi} F_{fe} \zeta_{f_{1s}} + (f_B F_{fa} + f_B F'_{fa}) \zeta_{f_{1q}} \right) + [C_2] \left(M_{nfe} \zeta_{f_{1s}} + (M_{nfa} + M'_{nfa}) \right. \right. \\
& \cdot \zeta_{f_{1q}} \left. \right) \left. \right\} \lambda_u^s - \lambda_t^s \left\{ \frac{3}{2}[a_9 - a_7] f_{\pi} F_{fe} \zeta_{f_{1s}} + \frac{3}{2}[a_7 + a_9](f_B F_{fa} + f_B F'_{fa}) \zeta_{f_{1q}} + \frac{3}{2}C_{10} \right. \\
& \cdot \left(M_{nfe} \zeta_{f_{1s}} + (M_{nfa} + M'_{nfa}) \zeta_{f_{1q}} \right) + \frac{3}{2}[C_8] \left(M_{nfe}^{P_2} \zeta_{f_{1s}} + (M_{nfa}^{P_2} + M_{nfa}'^{P_2}) \zeta_{f_{1q}} \right) \left. \right\}; \tag{41}
\end{aligned}$$

$$\begin{aligned}
\mathcal{A}(B_s^0 \rightarrow f_1(1285)\bar{K}^0) = & \lambda_u^d \left\{ [a_2] f_{f_{1q}} F'_{fe} + [C_2] M'_{nfe} \right\} \zeta_{f_{1q}} - \lambda_t^d \left\{ [a_4 - \frac{1}{2}a_{10}] \left((f_K F_{fe} + f_B F_{fa}) \zeta_{f_{1s}} + f_B F'_{fa} \right. \right. \\
& \cdot \zeta_{f_{1q}} \left. \right) + [a_6 - \frac{1}{2}a_8] \left((f_K F_{fe}^{P_2} + f_B F_{fa}^{P_2}) \zeta_{f_{1s}} + f_B F_{fa}'^{P_2} \zeta_{f_{1q}} \right) + [C_3 - \frac{1}{2}C_9] \left(M'_{nfa} \zeta_{f_{1q}} \right. \\
& + (M_{nfe} + M_{nfa}) \zeta_{f_{1s}} \left. \right) + [C_5 - \frac{1}{2}C_7] \left((M_{nfe}^{P_1} + M_{nfa}^{P_1}) \zeta_{f_{1s}} + M_{nfa}'^{P_1} \zeta_{f_{1q}} \right) + \left([2a_3 \right. \\
& + a_4 - 2a_5 - \frac{1}{2}(a_7 - a_9 + a_{10})] f_{f_{1q}} F'_{fe} + [C_3 + 2C_4 - \frac{1}{2}(C_9 - C_{10})] M'_{nfe} + [C_5 \\
& - \frac{1}{2}C_7] M_{nfe}'^{P_1} + [2C_6 + \frac{1}{2}C_8] M_{nfe}'^{P_2} \left. \right) \zeta_{f_{1q}} + \left([a_3 - a_5 + \frac{1}{2}(a_7 - a_9)] f_{f_{1s}} F'_{fe} + [C_4 \right. \\
& \left. - \frac{1}{2}C_{10}] M'_{nfe} + [C_6 - \frac{1}{2}C_8] M_{nfe}'^{P_2} \right) \zeta_{f_{1s}} \left. \right\}; \tag{42}
\end{aligned}$$

$$\begin{aligned}
\mathcal{A}(B_s^0 \rightarrow f_1(1285)\eta) = & \lambda_u^s \left\{ \zeta_{f_{1s}} \cdot \zeta_{\eta_q} ([a_2] f_{\eta_q} F_{fe} + [C_2] M_{nfe}) + \zeta_{\eta_s} \cdot \zeta_{f_{1q}} ([a_2] f_{f_{1s}} F'_{fe} + [C_2] M'_{nfe}) + \zeta_{\eta_q} \cdot \zeta_{f_{1q}} \right. \\
& \cdot \left([a_2] (f_B F_{fa} + f_B F'_{fa}) + [C_2] (M_{nfa} + M'_{nfa}) \right) \left. \right\} - \lambda_t^s \left\{ \zeta_{\eta_s} \cdot \zeta_{f_{1s}} \left((a_3 + a_4 - a_5 + \frac{1}{2} \right. \right. \\
& \cdot (a_7 - a_9 - a_{10})) (f_{\eta_s} F_{fe} + f_{1s} F'_{fe}) + (a_6 - \frac{1}{2} a_8) (f_{\eta_s} F_{fe}^{P_2} + f_B F_{fa}^{P_2} + f_B F_{fa}'^{P_2}) + (C_3 \\
& + C_4 - \frac{1}{2} (C_9 + C_{10})) (M_{nfe} + M'_{nfe} + M_{nfa} + M'_{nfa}) + (C_5 - \frac{1}{2} C_7) (M_{nfe}^{P_1} + M_{nfe}'^{P_1} \\
& + M_{nfa}^{P_1} + M_{nfa}'^{P_1}) + (C_6 - \frac{1}{2} C_8) (M_{nfe}^{P_2} + M_{nfe}'^{P_2} + M_{nfa}^{P_2} + M_{nfa}'^{P_2}) + (a_3 + a_4 + a_5 \\
& - \frac{1}{2} (a_7 + a_9 + a_{10})) (f_B F_{fa} + f_B F'_{fa}) \left. \right) + \zeta_{\eta_q} \cdot \zeta_{f_{1q}} \left((2C_4 + \frac{1}{2} C_{10}) (M_{nfa} + M'_{nfa}) \right. \\
& + (2C_6 + \frac{1}{2} C_8) (M_{nfa}^{P_2} + M_{nfa}'^{P_2}) + (2a_3 + 2a_5 + \frac{1}{2} (a_7 + a_9)) (f_B F_{fa} + f_B F'_{fa}) \left. \right) + \zeta_{f_{1s}} \\
& \cdot \zeta_{\eta_q} \left((2a_3 - 2a_5 - \frac{1}{2} (a_7 - a_9)) f_{\eta_q} F_{fe} + (2C_4 + \frac{1}{2} C_{10}) M_{nfe} + (2C_6 + \frac{1}{2} C_8) M_{nfe}^{P_2} \right) \\
& \left. + \zeta_{\eta_s} \cdot \zeta_{f_{1q}} \left((2a_3 - 2a_5 - \frac{1}{2} (a_7 - a_9)) f_{1s} F'_{fe} + (2C_4 + \frac{1}{2} C_{10}) M'_{nfe} + (2C_6 + \frac{1}{2} C_8) M_{nfe}'^{P_2} \right) \right\}
\end{aligned}$$

$$\begin{aligned}
\mathcal{A}(B_s^0 \rightarrow f_1(1285)\eta') = & \lambda_u^s \left\{ \zeta_{f_{1s}} \cdot \zeta'_{\eta_q} ([a_2] f_{\eta_q} F_{fe} + [C_2] M_{nfe}) + \zeta'_{\eta_s} \cdot \zeta_{f_{1q}} ([a_2] f_{f_{1s}} F'_{fe} + [C_2] M'_{nfe}) + \zeta'_{\eta_q} \cdot \zeta_{f_{1q}} \right. \\
& \cdot \left([a_2] (f_B F_{fa} + f_B F'_{fa}) + [C_2] (M_{nfa} + M'_{nfa}) \right) \left. \right\} - \lambda_t^s \left\{ \zeta'_{\eta_s} \cdot \zeta_{f_{1s}} \left((a_3 + a_4 - a_5 + \frac{1}{2} \right. \right. \\
& \cdot (a_7 - a_9 - a_{10})) (f_{\eta_s} F_{fe} + f_{1s} F'_{fe}) + (a_6 - \frac{1}{2} a_8) (f_{\eta_s} F_{fe}^{P_2} + f_B F_{fa}^{P_2} + f_B F_{fa}'^{P_2}) + (C_3 \\
& + C_4 - \frac{1}{2} (C_9 + C_{10})) (M_{nfe} + M'_{nfe} + M_{nfa} + M'_{nfa}) + (C_5 - \frac{1}{2} C_7) (M_{nfe}^{P_1} + M_{nfe}'^{P_1} \\
& + M_{nfa}^{P_1} + M_{nfa}'^{P_1}) + (C_6 - \frac{1}{2} C_8) (M_{nfe}^{P_2} + M_{nfe}'^{P_2} + M_{nfa}^{P_2} + M_{nfa}'^{P_2}) + (a_3 + a_4 + a_5 - \frac{1}{2} \\
& \cdot (a_7 + a_9 + a_{10})) (f_B F_{fa} + f_B F'_{fa}) \left. \right) + \zeta'_{\eta_q} \cdot \zeta_{f_{1q}} \left((2C_4 + \frac{1}{2} C_{10}) (M_{nfa} + M'_{nfa}) + (2C_6 \right. \\
& + \frac{1}{2} C_8) (M_{nfa}^{P_2} + M_{nfa}'^{P_2}) + (2a_3 + 2a_5 + \frac{1}{2} (a_7 + a_9)) (f_B F_{fa} + f_B F'_{fa}) \left. \right) + \zeta_{f_{1s}} \cdot \zeta'_{\eta_q} \left((2a_3 \right. \\
& - 2a_5 - \frac{1}{2} (a_7 - a_9)) f_{\eta_q} F_{fe} + (2C_4 + \frac{1}{2} C_{10}) M_{nfe} + (2C_6 + \frac{1}{2} C_8) M_{nfe}^{P_2} \left. \right) + \zeta'_{\eta_s} \cdot \zeta_{f_{1q}} \left((2a_3 \right. \\
& - 2a_5 - \frac{1}{2} (a_7 - a_9)) f_{1s} F'_{fe} + (2C_4 + \frac{1}{2} C_{10}) M'_{nfe} + (2C_6 + \frac{1}{2} C_8) M_{nfe}'^{P_2} \left. \right) \left. \right\}; \quad (44)
\end{aligned}$$

where $\lambda_u^{d(s)} = V_{ub}^* V_{ud(s)}$ and $\lambda_t^{d(s)} = V_{tb}^* V_{td(s)}$, $\zeta_{f_{1q}} = \cos \phi_{f_1} / \sqrt{2}$ and $\zeta_{f_{1s}} = -\sin \phi_{f_1}$, $\zeta_{\eta_q} = \cos \phi / \sqrt{2}$ and $\zeta_{\eta_s} = -\sin \phi$, and $\zeta'_{\eta_q} = \sin \phi / \sqrt{2}$ and $\zeta'_{\eta_s} = \cos \phi$. When we make the replacements with $\zeta_{f_{1q}} \rightarrow \zeta'_{f_{1q}} \sim \sin \phi_{f_1} / \sqrt{2}$ and $\zeta_{f_{1s}} \rightarrow \zeta'_{f_{1s}} \sim \cos \phi_{f_1}$ in the above equations, i.e., Eqs. (35)-(44), the decay amplitudes of $B \rightarrow f_1(1420)P$ modes will be easily obtained.

III. NUMERICAL RESULTS AND DISCUSSIONS

In this section, we will present the theoretical predictions on the CP -averaged branching ratios and CP -violating asymmetries for the considered 20 $B \rightarrow f_1 P$ decay modes in the pQCD approach. In numerical calculations, central values of the input parameters will be used implicitly unless otherwise stated. The relevant QCD scale (GeV), masses (GeV), and B meson

lifetime(ps) are the following [10, 11, 37, 51]:

$$\begin{aligned}
\Lambda_{\overline{\text{MS}}}^{(f=4)} &= 0.250, \quad m_W = 80.41, \quad m_B = 5.28, \quad m_{B_s} = 5.37, \quad m_b = 4.8; \\
f_\pi &= 0.13, \quad f_K = 0.16, \quad m_{f_1(1285)} = 1.2812, \quad m_{f_1(1420)} = 1.4264; \\
m_0^\pi &= 1.4, \quad m_0^K = 1.6, \quad m_0^{\eta_q} = 1.08, \quad m_0^{\eta_s} = 1.92, \quad \phi_{f_1} = 24.0^\circ; \\
\tau_{B_u} &= 1.641, \quad \tau_{B_d} = 1.519, \quad \tau_{B_s} = 1.497.
\end{aligned} \tag{45}$$

For the CKM matrix elements, we adopt the Wolfenstein parametrization and the updated parameters $A = 0.811$, $\lambda = 0.22535$, $\bar{\rho} = 0.131^{+0.026}_{-0.013}$, and $\bar{\eta} = 0.345^{+0.013}_{-0.014}$ [51].

A. CP -averaged branching ratios of $B \rightarrow f_1 P$ decays in the pQCD approach

For the considered $B \rightarrow f_1 P$ decays, the decay rate can be written as

$$\Gamma = \frac{G_F^2 m_B^3}{32\pi} (1 - r_{f_1}^2) |\mathcal{A}(B \rightarrow f_1 P)|^2, \tag{46}$$

where the corresponding decay amplitudes \mathcal{A} have been given explicitly in Eqs. (35)~(44). Using the decay amplitudes obtained in the last section, it is straightforward to calculate the CP -averaged branching ratios with uncertainties for the considered decay modes in the pQCD approach. The pQCD predictions for the CP -averaged branching ratios of the considered $B \rightarrow f_1 P$ decays have been collected in Tables I and II. Based on these numerical results, some phenomenological discussions are given in order:

TABLE I. The CP -averaged branching ratios for $B^+ \rightarrow f_1(\pi^+, K^+)$ decays in the pQCD approach.

Channels	CP -averaged branching ratios
$B^+ \rightarrow f_1(1285)\pi^+$	$4.0^{+1.1}_{-0.8}(\omega_b)^{+1.9}_{-1.4}(f_{f_1})^{+2.2}_{-1.7}(a_i^M)^{+0.2}_{-0.2}(\phi_{f_1})^{+0.1}_{-0.1}(a_t) \times 10^{-6}$
$B^+ \rightarrow f_1(1420)\pi^+$	$7.4^{+2.0}_{-1.5}(\omega_b)^{+3.6}_{-2.6}(f_{f_1})^{+4.1}_{-3.2}(a_i^M)^{+1.9}_{-1.5}(\phi_{f_1})^{+0.2}_{-0.2}(a_t) \times 10^{-7}$
$B^+ \rightarrow f_1(1285)K^+$	$1.6^{+0.4}_{-0.3}(\omega_b)^{+1.2}_{-0.8}(f_{f_1})^{+1.8}_{-1.1}(a_i^M)^{+0.2}_{-0.3}(\phi_{f_1})^{+0.1}_{-0.1}(a_t) \times 10^{-6}$
$B^+ \rightarrow f_1(1420)K^+$	$5.1^{+1.0}_{-0.8}(\omega_b)^{+0.9}_{-0.7}(f_{f_1})^{+1.4}_{-1.2}(a_i^M)^{+0.3}_{-0.3}(\phi_{f_1})^{+0.7}_{-0.6}(a_t) \times 10^{-6}$

- (1) The theoretical errors of these predictions in the pQCD approach are induced mainly by the uncertainties of the shape parameters $\omega_b = 0.40 \pm 0.04$ ($\omega_b = 0.50 \pm 0.05$) GeV for the $B_{u,d}$ (B_s) meson wave function, of the combined f_{f_1} from the axial-vector $f_{1q(s)}$ state decay constant $f_{f_1 q} = 0.193^{+0.043}_{-0.038}$ ($f_{f_1 s} = 0.230 \pm 0.009$) GeV, of the combined Gegenbauer moments a_i^M from $a_i^{\parallel, \perp}$ ($i = 1, 2$) for the axial-vector $f_{1q(s)}$ states in the longitudinal polarization and $a_{(1)2}^P$ for the pseudoscalar P meson, and of the mixing angle $\phi_{f_1} = (24.0^{+3.2}_{-2.7})^\circ$, respectively. Note that very small effects induced by the variation of the CKM parameters appear in the CP -averaged branching ratios of these considered $B \rightarrow f_1 P$ decays and thus have been safely neglected. Furthermore, we also investigate the higher order contributions simply through exploring the variation of the hard scale t_{\max} , i.e., from $0.8t$ to $1.2t$ (not changing $1/b_i$, $i = 1, 2, 3$), in the hard kernel, which have been counted into one of the sources of theoretical uncertainties. One can clearly observe that some penguin-dominated decays such as $B^+ \rightarrow f_1(1420)K^+$, $B_d^0 \rightarrow f_1(1420)K^0$, $B_s^0 \rightarrow f_1\bar{K}^0$, and $B_{d/s}^0 \rightarrow f_1\eta^{(\prime)}$ channels get large higher order corrections around 15% ~ 40% to the CP -averaged branching ratios as presented in the Tables I~II.
- (2) The considered $B \rightarrow f_1 P$ decays can be classified into two kinds of transitions, i.e., $b \rightarrow d(\Delta S = 0)$ and $b \rightarrow s(\Delta S = 1)$, respectively. The former transition includes ten $B_{u,d} \rightarrow f_1(\pi, \eta, \eta')$ and $B_s \rightarrow f_1\bar{K}^0$ modes, while the latter transition contains the other ten $B_{u,d} \rightarrow f_1 K$ and $B_s \rightarrow f_1(\pi^0, \eta, \eta')$ channels.
 - (a) For $\Delta S = 0$ decays, it is found that most of the branching ratios are in the order of $10^{-8} \sim 10^{-7}$ in the pQCD approach, except for the $B^+ \rightarrow f_1\pi^+$ modes with the decay rates as

$$Br(B^+ \rightarrow f_1(1285)\pi^+) \approx 4.0^{+3.1}_{-2.4} \times 10^{-6}, \quad Br(B^+ \rightarrow f_1(1420)\pi^+) \approx 0.7^{+0.6}_{-0.5} \times 10^{-6}; \tag{47}$$

which are around $\mathcal{O}(10^{-6})$ within large errors, where various errors as specified previously have been added in quadrature. It is noted that these two $B^+ \rightarrow f_1\pi^+$ decays are dominated by the color-allowed tree amplitudes, while the other eight $B_{d/s}^0 \rightarrow f_1(\pi^0, \eta, \eta')/\bar{K}^0$ processes are basically penguin dominant with color-suppressed tree

contributions. In particular, for the $B_s^0 \rightarrow f_1 \bar{K}^0$ channels, the tree pollution is so tiny that it can be neglected safely for the predictions of the CP -averaged branching ratios.

- (b) For $\Delta S = 1$ decays, contrary to the $\Delta S = 0$ ones, it is observed that most of the branching ratios are in the order of $10^{-6} \sim 10^{-5}$ in the pQCD approach, apart from the $B_s^0 \rightarrow f_1 \pi^0$ channels with the decay rates as

$$Br(B_s^0 \rightarrow f_1(1285)\pi^0) \approx 2.7_{-1.6}^{+2.0} \times 10^{-8}, \quad Br(B_s^0 \rightarrow f_1(1420)\pi^0) \approx 1.4_{-0.7}^{+1.0} \times 10^{-7}; \quad (48)$$

in which the theoretical errors from the input parameters have also been added in quadrature. In contrast to the above case, it is worthwhile to stress that all of the $b \rightarrow s$ transition processes are determined by the penguin contributions dramatically just with generally very small tree contaminations.

The relation of the CP -averaged branching ratios between these two $\Delta S = 0$ and $\Delta S = 1$ transitions can be understood naively through the involved CKM hierarchy [3], apart from the the interferences between $f_{1q}P$ and $f_{1s}P$ states, $|\lambda_u^d| : |\lambda_u^s| : |\lambda_t^d| : |\lambda_t^s| \sim 0.09 : 0.02 : 0.22 : 1$, which means that when the decays are dominated by the penguin contributions, then we must observe at least one order difference as roughly anticipated because of the value around 21 of $|\lambda_t^s/\lambda_t^d|^2$. It is known that the $B_d^0 \rightarrow K^+K^-$ with decay rate $1.3 \pm 0.5 \times 10^{-7}$ and the $B_s^0 \rightarrow \pi^+\pi^-$ with branching ratio $7.6 \pm 1.9 \times 10^{-7}$ have been detected by the experiments [3]. Therefore, the decay modes with the branching ratios in the order of 10^{-6} and larger are generally expected to be accessed more easily at the running LHCb and forthcoming Belle II experiments in the near future.

- (3) By careful analysis on the decay amplitudes, it is found that the $B^+ \rightarrow f_1 \pi^+ (\Delta S = 0)$ decays are almost dominated by the contributions from factorizable emission diagrams. Moreover, based on Eqs. (34), (35), and (37), and the numerical results of the branching ratios in Table I, one can straightforwardly see the constructive (destructive) effects to the $B_{u,d} \rightarrow f_1(1285)\pi$ [$f_1(1420)\pi$] decays.

Theoretically, these four decays have also been studied in the QCDF,³ and the numerical results can be read as (in units of 10^{-6}) [14]

$$Br(B^+ \rightarrow f_1(1285)\pi^+) = \begin{cases} 5.2_{-1.0}^{+1.5} \\ 4.6_{-0.9}^{+1.3} \end{cases}, \quad Br(B^0 \rightarrow f_1(1285)\pi^0) = \begin{cases} 0.26_{-0.11}^{+0.32} \\ 0.20_{-0.09}^{+0.27} \end{cases}; \quad (49)$$

$$Br(B^+ \rightarrow f_1(1420)\pi^+) = \begin{cases} 0.06_{-0.003}^{+0.01} \\ 0.59_{-0.15}^{+0.21} \end{cases}, \quad Br(B^0 \rightarrow f_1(1420)\pi^0) = \begin{cases} 0.003_{-0.003}^{+0.005} \\ 0.05_{-0.03}^{+0.05} \end{cases}. \quad (50)$$

Note that the predictions of the branching ratios for $B_{u,d} \rightarrow f_1 \pi$ decays in the QCDF correspond to two different sets of θ_{3P_1} in the flavor singlet-octet basis, i.e., 27.9° (first entry) and 53.2° (second entry). One can easily find the good agreement between the pQCD predictions with $\phi_{f_1} \sim 24^\circ$ and the QCDF predictions with $\theta_{3P_1} \sim 53.2^\circ$ for the $B_{u,d} \rightarrow f_1 \pi$ decays within errors.

TABLE II. Same as Table I but for $B_{d/s}^0 \rightarrow f_1(\pi^0, K^0, \eta, \eta')$ decays.

Channels	CP -averaged branching ratios	Channels	CP -averaged branching ratios
$B_d^0 \rightarrow f_1(1285)\pi^0$	$1.4_{-0.3-0.4-0.3-0.0-0.2}^{+0.4+0.6+0.5+0.0+0.2} \times 10^{-7}$	$B_s^0 \rightarrow f_1(1285)\pi^0$	$2.7_{-0.7-0.2-1.3-0.5-0.2}^{+0.9+0.2+1.6+0.7+0.3} \times 10^{-8}$
$B_d^0 \rightarrow f_1(1420)\pi^0$	$1.1_{-0.1-0.3-0.1-0.2-0.1}^{+0.0+0.6+0.4+0.3+0.1} \times 10^{-8}$	$B_s^0 \rightarrow f_1(1420)\pi^0$	$1.4_{-0.4-0.1-0.6-0.1-0.1}^{+0.5+0.1+0.8+0.1+0.1} \times 10^{-7}$
$B_d^0 \rightarrow f_1(1285)K^0$	$1.8_{-0.4-0.8-1.4-0.3-0.2}^{+0.5+1.3+2.1+0.3+0.2} \times 10^{-6}$	$B_s^0 \rightarrow f_1(1285)\bar{K}^0$	$7.4_{-1.8-0.6-4.5-1.5-1.1}^{+2.7+0.6+6.6+2.0+2.5} \times 10^{-8}$
$B_d^0 \rightarrow f_1(1420)K^0$	$4.8_{-0.8-0.7-1.2-0.3-0.5}^{+1.0+0.9+1.4+0.3+0.7} \times 10^{-6}$	$B_s^0 \rightarrow f_1(1420)\bar{K}^0$	$5.9_{-1.4-0.5-2.9-0.2-0.8}^{+2.0+0.5+3.9+0.1+1.1} \times 10^{-7}$
$B_d^0 \rightarrow f_1(1285)\eta$	$1.0_{-0.1-0.4-0.1-0.0-0.1}^{+0.2+0.5+0.2+0.0+0.3} \times 10^{-7}$	$B_s^0 \rightarrow f_1(1285)\eta$	$3.9_{-1.0-0.4-1.2-0.7-0.9}^{+1.6+0.4+1.3+0.8+1.5} \times 10^{-6}$
$B_d^0 \rightarrow f_1(1420)\eta$	$1.7_{-0.2-0.6-0.7-0.4-0.0}^{+0.2+0.9+0.9+0.5+0.1} \times 10^{-8}$	$B_s^0 \rightarrow f_1(1420)\eta$	$1.3_{-0.3-0.1-0.4-0.1-0.2}^{+0.4+0.1+0.5+0.1+0.3} \times 10^{-5}$
$B_d^0 \rightarrow f_1(1285)\eta'$	$3.3_{-0.1-1.2-1.1-0.2-0.2}^{+0.2+1.8+1.6+0.2+0.9} \times 10^{-8}$	$B_s^0 \rightarrow f_1(1285)\eta'$	$3.4_{-0.9-0.4-0.4-0.5-0.6}^{+1.3+0.5+0.4+0.6+0.9} \times 10^{-6}$
$B_d^0 \rightarrow f_1(1420)\eta'$	$5.0_{-0.6-0.6-2.0-0.2-0.8}^{+0.9+0.8+2.6+0.2+1.0} \times 10^{-8}$	$B_s^0 \rightarrow f_1(1420)\eta'$	$1.1_{-0.2-0.1-0.1-0.1-0.2}^{+0.2+0.1+0.1+0.1+0.3} \times 10^{-5}$

³ As stressed in the Introduction, the branching ratios of the $B \rightarrow f_1 P$ decays given in the naive factorization are very crude. Thus we will only compare our predictions with that obtained in the QCDF theoretically.

According to Ref. [47], the mixing of the $f_1(1285) - f_1(1420)$ system in the singlet-octet and quark-flavor bases can be written as the following form,

$$\begin{pmatrix} |f_1(1285)\rangle \\ |f_1(1420)\rangle \end{pmatrix} = \begin{pmatrix} \cos \theta_{3P_1} & \sin \theta_{3P_1} \\ -\sin \theta_{3P_1} & \cos \theta_{3P_1} \end{pmatrix} \begin{pmatrix} |f_1\rangle \\ |f_8\rangle \end{pmatrix} = \begin{pmatrix} \cos \alpha_{3P_1} & \sin \alpha_{3P_1} \\ -\sin \alpha_{3P_1} & \cos \alpha_{3P_1} \end{pmatrix} \begin{pmatrix} |f_{1q}\rangle \\ |f_{1s}\rangle \end{pmatrix}, \quad (51)$$

where f_1 and f_8 are the flavor singlet and flavor octet, respectively, and the mixing angle α_{3P_1} in the quark-flavor basis satisfies the relation $\alpha_{3P_1} = 35.3^\circ - \theta_{3P_1}$ and measures the deviation from ideal mixing. Then the $\alpha_{3P_1} \sim -17.9^\circ$ can be derived from the second entry in the QCDF, which thus leads to the same mixing form as that adopted in this work, i.e., Eq. (34) with a positive value of the mixing angle.

Furthermore, a reasonable deduction obtained more naturally is that the $f_1(1285)$ [$f_1(1420)$] is basically determined by the component f_{1q} [f_{1s}] based on the following ratios(central values) between the branching ratios of $B^+ \rightarrow f_1\pi^+$ decays in the pQCD and QCDF approaches,

$$R_{f_1(1285)\pi} \equiv \frac{Br(B^+ \rightarrow f_1(1285)\pi^+)_{\text{QCDF}}}{Br(B^+ \rightarrow f_1(1285)\pi^+)_{\text{pQCD}}} \approx 1.15 \sim \left| \frac{\cos \alpha_{3P_1}}{\cos \phi_{f_1}} \right|^2 \approx 1.09, \quad (52)$$

$$R_{f_1(1420)\pi} \equiv \frac{Br(B^+ \rightarrow f_1(1420)\pi^+)_{\text{QCDF}}}{Br(B^+ \rightarrow f_1(1420)\pi^+)_{\text{pQCD}}} \approx 0.80 \sim \left| \frac{\sin \alpha_{3P_1}}{\sin \phi_{f_1}} \right|^2 \approx 0.58. \quad (53)$$

Notice that the above relations cannot be easily deduced from the $B_d^0 \rightarrow f_1\pi^0$ modes. The underlying reason is that the former $B^+ \rightarrow f_1\pi^+$ decays are with the dominant tree(color-allowed) contributions and negligible penguin pollution, while the latter $B_d^0 \rightarrow f_1\pi^0$ channels embrace the small tree(color-suppressed) and more important penguin contributions. The predictions of the CP -averaged branching ratios for $B_{u,d} \rightarrow f_1\pi$ decays in the pQCD approach with the corresponding phenomenological discussions are expected to be tested by the near future experiments at LHC.

- (4) For the penguin-dominated $B_{u,d} \rightarrow f_1K$ decays, the destructive (constructive) interferences between $f_{1q}K$ and $f_{1s}K$ result in the approximately equal branching ratios for $B_{u,d} \rightarrow f_1(1285)K$ [$f_1(1420)K$] decays,

$$Br(B^+ \rightarrow f_1(1285)K^+) = 1.6_{-1.4}^{+2.2} \times 10^{-6} \sim Br(B_d^0 \rightarrow f_1(1285)K^0) = 1.8_{-1.7}^{+2.5} \times 10^{-6}, \quad (54)$$

$$Br(B^+ \rightarrow f_1(1420)K^+) = 5.1_{-1.7}^{+2.1} \times 10^{-6} \sim Br(B_d^0 \rightarrow f_1(1420)K^0) = 4.8_{-1.7}^{+2.1} \times 10^{-6}, \quad (55)$$

which indicate that the tree contributions are highly suppressed because of $|\lambda_u^s| : |\lambda_t^s| \sim 0.02$. Of course, it is worth stressing that, in terms of the central values of the decay rates, the color-allowed tree contributions(around 10%) of $B^+ \rightarrow f_1K^+$ decays are larger than those color-suppressed ones (almost 0%) of $B_d^0 \rightarrow f_1K^0$ decays, though which are negligible relative to dominant penguin contributions in both sets of decay modes.

The predictions on the branching ratios have also been presented in the framework of QCDF(in units of 10^{-6}) [14]:

$$Br(B^+ \rightarrow f_1(1285)K^+) = 5.2_{-10.1}^{+9.7}, \quad Br(B^+ \rightarrow f_1(1420)K^+) = 13.8_{-7.8}^{+18.4}, \quad (56)$$

$$Br(B_d^0 \rightarrow f_1(1285)K^0) = 5.2_{-2.2}^{+4.5}, \quad Br(B_d^0 \rightarrow f_1(1420)K^0) = 13.1_{-7.3}^{+17.5}. \quad (57)$$

In view of the better consistency observed from the $B_{u,d} \rightarrow f_1\pi$ decays theoretically, we here only quote the second entry of the branching ratios for $B_{u,d} \rightarrow f_1K$ decays in the QCDF for clarification. It can be seen that the theoretical predictions in both pQCD and QCDF approaches are basically consistent with each other within still large uncertainties. However, as far as the central values are considered, $Br(B_{u,d} \rightarrow f_1K)_{\text{QCDF}}$ are a bit larger than $Br(B_{u,d} \rightarrow f_1K)_{\text{pQCD}}$ with a factor near 3.

As mentioned in the Introduction, there are just the preliminary upper limits of branching ratios for the $B^+ \rightarrow f_1K^+$ decays made by the BABAR Collaboration [13],

$$Br(B^+ \rightarrow f_1(1285)K^+) < 2.0 \times 10^{-6}, \quad (58)$$

and

$$Br(B^+ \rightarrow f_1(1420)K^+) \cdot Br(f_1(1420) \rightarrow \bar{K}^*K) < 4.1 \times 10^{-6}, \quad (59)$$

$$Br(B^+ \rightarrow f_1(1420)K^+) \cdot Br(f_1(1420) \rightarrow \eta\pi\pi) < 2.9 \times 10^{-6}. \quad (60)$$

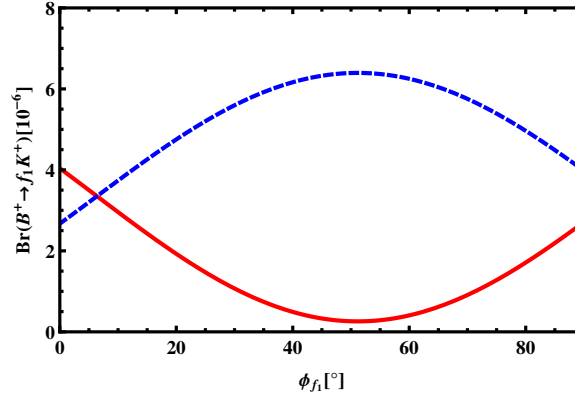


FIG. 2. (Color online) Dependence on the mixing angle ϕ_{f_1} of the branching ratios of $B^+ \rightarrow f_1 K^+$ in the pQCD approach. The red solid [blue dashed] line corresponds to the $B^+ \rightarrow f_1(1285)K^+$ [$f_1(1420)K^+$] decay, respectively.

We can find that the prediction for $Br(B^+ \rightarrow f_1(1285)K^+)$ in the pQCD approach is in good agreement with the preliminary upper limit, while that in the QCDF is barely consistent with the experimental limit within large theoretical errors. There are no accurate values of the decay rates of $f_1(1420) \rightarrow \bar{K}^* K$ and $\eta\pi\pi$ modes currently, which consequently results in no available upper bound for $B^+ \rightarrow f_1(1420)K^+$ channel. But, it can be imagined that we can extract phenomenologically the information on the decay rates of $f_1(1420) \rightarrow \bar{K}^* K$ and $\eta\pi\pi$ decays if our predictions of $Br(B^+ \rightarrow f_1(1420)K^+) \sim \mathcal{O}(10^{-6})$ are confirmed by the measurements at LHCb and Belle II experiments in the near future. Of course, we first need to await enough data samples to test our theoretical predictions.

In order to observe the dependence on the mixing angle ϕ_{f_1} of the $B^+ \rightarrow f_1 K^+$ decays, we simply examine the central values of the branching ratios in the pQCD approach as a function of ϕ_{f_1} in the range of $[0, 90^\circ]$, which can be seen in Fig. 2. One can observe that the ϕ_{f_1} dependence of the $B^+ \rightarrow f_1(1420)K^+$ mode is opposite to that of the $B^+ \rightarrow f_1(1285)K^+$ directly from Fig. 2. Moreover, we also present the branching ratios of $B^+ \rightarrow f_1 K^+$ decays in the pQCD approach with $\phi_{f_1} \sim 15^\circ$ and 20° as a reference:

$$Br(B^+ \rightarrow f_1(1285)K^+) = 2.4^{+2.9}_{-1.9} \times 10^{-6}, \quad Br(B^+ \rightarrow f_1(1420)K^+) = 4.3^{+1.6}_{-1.4} \times 10^{-6}, \quad (61)$$

with $\phi_{f_1} \sim 15^\circ$ and

$$Br(B^+ \rightarrow f_1(1285)K^+) = 1.9^{+2.6}_{-1.6} \times 10^{-6}, \quad Br(B^+ \rightarrow f_1(1420)K^+) = 4.8^{+1.7}_{-1.7} \times 10^{-6}, \quad (62)$$

with $\phi_{f_1} \sim 20^\circ$. According to the brief review of the $f_1(1285) - f_1(1420)$ mixing in the last section, in terms of the central values of the currently existing mixing angle ϕ_{f_1} from both theoretical and experimental sides, one can find that the angle ϕ_{f_1} lies in the range of $[15^\circ, 27^\circ]$ [47]. Similarly, if the preliminary upper limit for the branching ratio of the $B^+ \rightarrow f_1(1285)K^+$ mode could be considered as the central value of the experimental measurement, then we can find a rough constraint of the mixing angle ϕ_{f_1} through the numerical evaluations in the pQCD approach, i.e., $\phi_{f_1} \in [20^\circ, 27^\circ]$.

- (5) The CP -averaged branching ratios of $B_d^0 \rightarrow f_1(\eta, \eta')$ decays in the pQCD approach are presented in Table II. As a matter of fact, it is noted that these decays include two sets of destructive and/or constructive effects simultaneously due to $\eta - \eta'$ mixing and $f_1(1285) - f_1(1420)$ mixing. We find that $Br(B_d^0 \rightarrow f_1(1285)\eta) \sim 5 \times Br(B_d^0 \rightarrow f_1(1420)\eta)$ and $Br(B_d^0 \rightarrow f_1(1285)\eta') \sim Br(B_d^0 \rightarrow f_1(1420)\eta')$ within errors. While in terms of their central values of the branching ratios, we can easily find the constructive (destructive) interferences in $B_d^0 \rightarrow f_1(1285)\eta$ [$f_1(1420)\eta$] decays and the slightly destructive (constructive) effects in $B_d^0 \rightarrow f_1(1285)\eta'$ [$f_1(1420)\eta'$] ones. And the similarly interesting phenomena can be found correspondingly in $B_d^0 \rightarrow f_1(1285)\eta[\eta']$ and $B_d^0 \rightarrow f_1(1420)\eta[\eta']$ decays. Because of the similar behavior in both vector and axial-vector mesons and this interesting pattern also occurring in the $B_d^0 \rightarrow (\omega, \phi)(\eta, \eta')$ decays [43], it is reasonable to conjecture that the $f_1(1285)$ [$f_1(1420)$] is dominated by the f_{1q} [f_{1s}]. However, all magnitudes of these four branching ratios are so small that the current experiments cannot observe them in a short period, which then have to be detected in the future.
- (6) To our best knowledge, the $B_s^0 \rightarrow f_1 P$ decays are studied for the first time in the pQCD approach and their estimations on the physical observables such as CP -averaged branching ratios and CP -violating asymmetries have been collected in the Tables II and IV.

- (a) As shown in Table II, the CP -averaged branching ratios of $B_s^0 \rightarrow f_1(\pi^0, \bar{K}^0)$ decays are very small, around the order of $10^{-8} \sim 10^{-7}$ in the pQCD approach, which cannot be easily reached in the near future experiments. Relative to $B_d^0 \rightarrow f_1 K^0$ decays, the $B_s^0 \rightarrow f_1 \bar{K}^0$ ones are also the penguin-dominated processes with dramatically small tree amplitudes through the $\Delta S = 0$ transitions. Due to the CKM hierarchy, the moduli of λ_t^d is just about 22% of that of λ_t^s , which consequently leads to $Br(B_s^0 \rightarrow f_1 \bar{K}^0) < Br(B_d^0 \rightarrow f_1 K^0)$ as naive expectations. Different from $B_d^0 \rightarrow f_1 \pi^0$ decays, the $B_s^0 \rightarrow f_1 \pi^0$ decays have no $B_s^0 \rightarrow \pi^0$ transitions and are nearly determined by the factorizable emission contributions via $B_s^0 \rightarrow f_{1s}$ transitions. Based on Eq. (34), the coefficients $-\sin \phi_{f_1}$ and $\cos \phi_{f_1}$ can be found in the $B_s^0 \rightarrow f_1(1285)\pi^0$ and $B_s^0 \rightarrow f_1(1420)\pi^0$ decays, respectively, which thus result in the smaller (larger) branching ratio of the former (latter) mode with $\sin^2(24^\circ) \sim 0.17$ [$\cos^2(24^\circ) \sim 0.83$]. The similar (contrary) decay pattern between $B_s^0 \rightarrow f_1 \bar{K}^0$ and $B_d^0 \rightarrow f_1 K^0$ [$B_s^0 \rightarrow f_1 \pi^0$ and $B_d^0 \rightarrow f_1 \pi^0$] modes can also clearly be seen from Table II.
- (b) The CP -averaged branching ratios of $B_s^0 \rightarrow f_1(\eta, \eta')$ modes completely dominated by the penguin contributions in the pQCD approach are large, in the order of $10^{-6} \sim 10^{-5}$, and are expected to be easily accessed by the ongoing LHCb and forthcoming Belle II experiments. Without the so-called tree contaminations, the central values of the decay rates of these four channels remain unchanged in the pQCD approach as presented in Table II. Similar to $B_d^0 \rightarrow f_1(\eta, \eta')$ decays, the $B_s^0 \rightarrow f_1(\eta, \eta')$ ones also embrace two sets of constructive and/or destructive interferences because of the $\eta_q - \eta_s$ mixing and $f_{1q} - f_{1s}$ mixing. But, in contrast to the decay pattern of $B_d^0 \rightarrow f_1(\eta, \eta')$, as far as the central values are considered, we find the weakly constructive (destructive) effects to the $B_s^0 \rightarrow f_1(1285)\eta[\eta']$ and $B_s^0 \rightarrow f_1(1420)\eta[\eta']$ decays, and the strongly destructive (constructive) interferences in the $B_s^0 \rightarrow f_1(1285)\eta[f_1(1420)\eta]$ and $B_s^0 \rightarrow f_1(1285)\eta'[f_1(1420)\eta']$ ones. By considering the theoretical errors, we can obtain the relations $Br(B_s^0 \rightarrow f_1(1285)\eta) \sim Br(B_s^0 \rightarrow f_1(1285)\eta') \sim \mathcal{O}(10^{-6})$ and $Br(B_s^0 \rightarrow f_1(1420)\eta) \sim Br(B_s^0 \rightarrow f_1(1420)\eta') \sim \mathcal{O}(10^{-5})$ approximately. It is therefore of great interest to examine these $B_s^0 \rightarrow f_1(\eta, \eta')$ decays, with 10^{-6} and even larger branching ratios, and interesting phenomenologies at the experimental aspects.
- (7) We also explore some ratios of the CP -averaged branching ratios of the considered $B \rightarrow f_1 P$ decays in the pQCD approach. For simplicity, we just present the ratios of decay modes with large branching ratios. Therefore, the relevant ratios can be read as follows:

$$R_1 \equiv \frac{Br(B^+ \rightarrow f_1(1420)\pi^+)}{Br(B^+ \rightarrow f_1(1285)\pi^+)} = 0.18_{-0.16}^{+0.20}, \quad (63)$$

$$R_2 \equiv \frac{Br(B^+ \rightarrow f_1(1285)K^+)}{Br(B^+ \rightarrow f_1(1420)K^+)} = 0.31_{-0.29}^{+0.45}, \quad (64)$$

$$R_3 \equiv \frac{Br(B_d^0 \rightarrow f_1(1285)K^0)}{Br(B_d^0 \rightarrow f_1(1420)K^0)} = 0.38_{-0.38}^{+0.55}, \quad (65)$$

$$R_4 \equiv \frac{Br(B_s^0 \rightarrow f_1(1285)\eta)}{Br(B_s^0 \rightarrow f_1(1420)\eta)} = 0.30_{-0.21}^{+0.26}, \quad (66)$$

$$R_5 \equiv \frac{Br(B_s^0 \rightarrow f_1(1285)\eta')}{Br(B_s^0 \rightarrow f_1(1420)\eta')} = 0.31_{-0.15}^{+0.20}. \quad (67)$$

One can directly observe that the ratio R_1 from $B^+ \rightarrow f_1 \pi^+(\Delta S = 0)$ is very different from the other four similar ratios R_{2-5} from $B_{u,d} \rightarrow f_1 K(\Delta S = 1)$ and $B_s^0 \rightarrow f_1(\eta, \eta')(\Delta S = 1)$. The measurements of these ratios will be helpful to understand the mixing angle ϕ_{f_1} of the $f_1(1285) - f_1(1420)$ system effectively and further determine the definite components of both f_1 mesons.

- (8) As mentioned in the Introduction, the contributions from weak annihilation diagrams play important roles in the heavy B meson decays, which are complex with a sizable strong phase proposed by the pQCD approach and supported by the QCDF approach through fitting to the data, although the contrary viewpoint has been stated by soft-collinear effective theory. We will therefore analyze the annihilation contributions in these 20 $B \rightarrow f_1 P$ decays. For the sake of simplicity, we here will only take the central values of the branching ratios in the pQCD approach for clarification.

- (a) For the $\Delta S = 0$ processes, when the weak annihilation contributions are neglected, then the branching ratios of the

ten $b \rightarrow d$ transitions can be presented as follows:

$$Br(B^+ \rightarrow f_1(1285)\pi^+) = 3.9 \times 10^{-6}, \quad Br(B^+ \rightarrow f_1(1420)\pi^+) = 7.1 \times 10^{-7}; \quad (68)$$

$$Br(B_d^0 \rightarrow f_1(1285)\pi^0) = 1.2 \times 10^{-7}, \quad Br(B_d^0 \rightarrow f_1(1420)\pi^0) = 2.1 \times 10^{-9}; \quad (69)$$

$$Br(B_d^0 \rightarrow f_1(1285)\eta) = 8.7 \times 10^{-8}, \quad Br(B_d^0 \rightarrow f_1(1420)\eta) = 5.1 \times 10^{-9}; \quad (70)$$

$$Br(B_d^0 \rightarrow f_1(1285)\eta') = 4.3 \times 10^{-9}, \quad Br(B_d^0 \rightarrow f_1(1420)\eta') = 4.3 \times 10^{-9}; \quad (71)$$

$$Br(B_s^0 \rightarrow f_1(1285)\bar{K}^0) = 5.5 \times 10^{-8}, \quad Br(B_s^0 \rightarrow f_1(1420)\bar{K}^0) = 5.3 \times 10^{-7}. \quad (72)$$

(b) For the $\Delta S = 1$ channels, when the weak annihilation contributions are turned off, then the decay rates of the ten $b \rightarrow s$ transitions can be given as follows:

$$Br(B^+ \rightarrow f_1(1285)K^+) = 1.8 \times 10^{-6}, \quad Br(B^+ \rightarrow f_1(1420)K^+) = 3.5 \times 10^{-6}; \quad (73)$$

$$Br(B_d^0 \rightarrow f_1(1285)K^0) = 2.0 \times 10^{-6}, \quad Br(B_d^0 \rightarrow f_1(1420)K^0) = 3.5 \times 10^{-6}; \quad (74)$$

$$Br(B_s^0 \rightarrow f_1(1285)\eta) = 4.2 \times 10^{-6}, \quad Br(B_s^0 \rightarrow f_1(1420)\eta) = 1.2 \times 10^{-5}; \quad (75)$$

$$Br(B_s^0 \rightarrow f_1(1285)\eta') = 3.4 \times 10^{-6}, \quad Br(B_s^0 \rightarrow f_1(1420)\eta') = 7.8 \times 10^{-6}; \quad (76)$$

$$Br(B_s^0 \rightarrow f_1(1285)\pi^0) = 2.7 \times 10^{-8}, \quad Br(B_s^0 \rightarrow f_1(1420)\pi^0) = 1.3 \times 10^{-7}. \quad (77)$$

Compared with the values listed in Tables I and II, one can find that the decays such as $B^+ \rightarrow f_1\pi^+$, $f_1(1285)K^+$, $B_d^0 \rightarrow f_1(1285)(\pi^0, K^0, \eta)$, and $B_s^0 \rightarrow f_1(1285)(\pi^0, \eta, \eta')$, $f_1(1420)(\pi^0, \bar{K}^0, \eta')$ are not significantly sensitive to the weak annihilation contributions. However, it is important to note that the modes such as $B_{u,d} \rightarrow f_1(1420)K$, $B_d^0 \rightarrow f_1(1285)\eta'$, $f_1(1420)(\pi^0, \eta, \eta')$, and $B_s^0 \rightarrow f_1(1285)\bar{K}^0$, $f_1(1420)\eta'$ suffer from sizable annihilation effects; specifically, without the contributions from annihilation diagrams, the branching ratios decrease correspondingly by around 30% for $B_{u,d} \rightarrow f_1(1420)K$ and $B_s^0 \rightarrow f_1(1420)\eta'$, 70% ~ 90% for $B_d^0 \rightarrow f_1\eta'$, $f_1(1420)(\pi^0, \eta)$, and 26% for $B_s^0 \rightarrow f_1(1285)\bar{K}^0$, respectively. Of course, the reliability of the contributions from the annihilation diagrams to these considered decays calculated in the pQCD approach will be carefully examined by the relevant experiments in the future.

(9) Frankly speaking, as the most important inputs in the calculations of pQCD approach, the currently less constrained light-cone distribution amplitudes of the axial-vector f_1 mesons result in the theoretical predictions of the branching ratios for the considered 20 $B \rightarrow f_1 P$ decays with relatively large uncertainties, which are expected to be greatly improved by the LQCD calculations and/or large numbers of related experiments in the future. For example, analogous to $\eta/\eta' \rightarrow \gamma\gamma$ [3, 52], one can fix the mixing angle ϕ_{f_1} and/or the decay constants of axial-vector f_1 mesons through the measurements on the decay widths of $f_1(1285)/f_1(1420) \rightarrow \gamma\gamma^*$ channels [49]. Of course, one can also determine the mixing angle ϕ_{f_1} through the Gell-Mann–Okubo mass formula for the 3P_1 axial-vector states, the relation of the decay rates of the radiative $f_1(1285) \rightarrow \rho\gamma$ and $\phi\gamma$ modes or of the radiative $J/\psi \rightarrow f_1(1285)\gamma$ and $f_1(1420)\gamma$ processes, and so on.

B. CP-violating asymmetries of $B \rightarrow f_1 P$ decays in the pQCD approach

TABLE III. The direct CP violations A_{CP}^{dir} for $B^+ \rightarrow f_1(\pi^+, K^+)$ decays in the pQCD approach. Apart from the last error induced by the variations of CKM parameters $\bar{\rho}$ and $\bar{\eta}$, the sources of the main uncertainties have been specified in the discussions of CP -averaged branching ratios.

Channels	direct CP violations(%)
$B^+ \rightarrow f_1(1285)\pi^+$	$18.3_{-1.9}^{+2.0}(\omega_b)_{-0.4}^{+0.3}(f_{f_1})_{-2.0}^{+3.3}(a_i^M)_{-0.2}^{+0.2}(\phi_{f_1})_{-2.0}^{+2.7}(a_t)_{-1.3}^{+0.7}(V_i)$
$B^+ \rightarrow f_1(1420)\pi^+$	$28.2_{-2.8}^{+2.8}(\omega_b)_{-1.4}^{+1.8}(f_{f_1})_{-4.0}^{+5.8}(a_i^M)_{-1.0}^{+1.1}(\phi_{f_1})_{-2.4}^{+2.7}(a_t)_{-1.7}^{+1.1}(V_i)$
$B^+ \rightarrow f_1(1285)K^+$	$-21.2_{-1.9}^{+1.6}(\omega_b)_{-1.9}^{+4.3}(f_{f_1})_{-24.0}^{+12.8}(a_i^M)_{-1.3}^{+2.4}(\phi_{f_1})_{-0.0}^{+0.1}(a_t)_{-1.3}^{+0.8}(V_i)$
$B^+ \rightarrow f_1(1420)K^+$	$-13.6_{-0.5}^{+0.6}(\omega_b)_{-1.3}^{+1.5}(f_{f_1})_{-2.0}^{+2.3}(a_i^M)_{-0.9}^{+0.9}(\phi_{f_1})_{-0.4}^{+0.5}(a_t)_{-0.5}^{+0.6}(V_i)$

Now we come to the evaluations of the CP -violating asymmetries of $B \rightarrow f_1 P$ decays in the pQCD approach. For the charged $B^+ \rightarrow f_1(\pi^+, K^+)$ decays, the direct CP violation A_{CP}^{dir} can be defined as,

$$A_{CP}^{\text{dir}} = \frac{|\bar{\mathcal{A}}_f|^2 - |\mathcal{A}_f|^2}{|\bar{\mathcal{A}}_f|^2 + |\mathcal{A}_f|^2}, \quad (78)$$

where \mathcal{A}_f stands for the decay amplitudes of $B^+ \rightarrow f_1\pi^+$ and $B^+ \rightarrow f_1K^+$, respectively, while $\overline{\mathcal{A}}_f$ denotes the charge conjugation $B^- \rightarrow f_1\pi^-$ and $B^- \rightarrow f_1K^-$ ones correspondingly. Using Eq. (78), the pQCD predictions for the direct CP -violating asymmetries of $B^+ \rightarrow f_1(\pi^+, K^+)$ modes have been collected in Table III, in which we can easily find the large direct CP violations for the four charged $B^+ \rightarrow f_1\pi^+$ and f_1K^+ decays within errors as follows:

$$A_{\text{CP}}^{\text{dir}}(B^+ \rightarrow f_1(1285)\pi^+) = (18.3_{-3.7}^{+4.8})\%, \quad A_{\text{CP}}^{\text{dir}}(B^+ \rightarrow f_1(1420)\pi^+) = (28.2_{-6.0}^{+7.4})\%; \quad (79)$$

$$A_{\text{CP}}^{\text{dir}}(B^+ \rightarrow f_1(1285)K^+) = (-21.2_{-24.2}^{+13.8})\%, \quad A_{\text{CP}}^{\text{dir}}(B^+ \rightarrow f_1(1420)K^+) = (-13.6_{-2.7}^{+3.1})\%, \quad (80)$$

where various errors from the variations of the input parameters have been added in quadrature. These large direct CP -violating asymmetries combined with the large CP -averaged branching ratios [$\mathcal{O}(10^{-6})$] are believed to be clearly measurable at the LHCb and Belle II experiments.

As for the CP -violating asymmetries for the neutral $B_{d(s)}^0 \rightarrow f_1P$ decays, the effects of $B_{d(s)}^0 - \bar{B}_{d(s)}^0$ mixing should be considered. The CP -violating asymmetries of $B_{d(s)}^0(\bar{B}_{d(s)}^0) \rightarrow f_1(\pi^0, K^0, \eta, \eta')$ decays are time dependent and can be defined as

$$A_{\text{CP}} \equiv \frac{\Gamma(\bar{B}_{d(s)}^0(\Delta t) \rightarrow f_{CP}) - \Gamma(B_{d(s)}^0(\Delta t) \rightarrow f_{CP})}{\Gamma(\bar{B}_{d(s)}^0(\Delta t) \rightarrow f_{CP}) + \Gamma(B_{d(s)}^0(\Delta t) \rightarrow f_{CP})} \\ = A_{\text{CP}}^{\text{dir}} \cos(\Delta m_{d(s)} \Delta t) + A_{\text{CP}}^{\text{mix}} \sin(\Delta m_{d(s)} \Delta t), \quad (81)$$

where $\Delta m_{d(s)}$ is the mass difference between the two $B_{d(s)}^0$ mass eigenstates, $\Delta t = t_{CP} - t_{\text{tag}}$ is the time difference between the tagged $B_{d(s)}^0$ [$\bar{B}_{d(s)}^0$] and the accompanying $\bar{B}_{d(s)}^0$ [$B_{d(s)}^0$] with opposite b flavor decaying to the final CP -eigenstate f_{CP} at

TABLE IV. The direct CP asymmetries $A_{\text{CP}}^{\text{dir}}$ (first entry) and the mixing-induced CP asymmetries $A_{\text{CP}}^{\text{mix}}$ (second entry) for $B_{d(s)}^0 \rightarrow f_1(\pi^0, K^0, \eta, \eta')$ decays in the pQCD approach. Moreover, the third entry in the right-hand side is for the observable $A_{\Delta\Gamma_s}$ in B_s^0 meson decays. Various errors arising from the input parameters as specified in previous section have been added in quadrature.

Channels	CP asymmetries(%)	Channels	CP asymmetries(%)
$B_d^0 \rightarrow f_1(1285)\pi^0$	$70.8_{-17.0}^{+12.5}$ $2.6_{-32.1}^{+38.9}$	$B_s^0 \rightarrow f_1(1285)\pi^0$	$-29.5_{-13.3}^{+10.7}$ $-9.9_{-12.0}^{+14.0}$ $95.0_{-4.4}^{+2.8}$
$B_d^0 \rightarrow f_1(1420)\pi^0$	$42.0_{-78.6}^{+51.8}$ $86.1_{-48.8}^{+13.6}$	$B_s^0 \rightarrow f_1(1420)\pi^0$	$14.3_{-6.9}^{+10.3}$ $-11.3_{-10.2}^{+12.3}$ $98.3_{-1.8}^{+1.0}$
$B_d^0 \rightarrow f_1(1285)K^0$	$2.3_{-1.3}^{+2.5}$ $70.0_{-2.9}^{+3.1}$	$B_s^0 \rightarrow f_1(1285)\bar{K}^0$	$26.0_{-30.0}^{+34.9}$ $-70.9_{-19.8}^{+36.3}$ $65.5_{-41.0}^{+28.7}$
$B_d^0 \rightarrow f_1(1420)K^0$	$0.6_{-0.5}^{+0.4}$ $69.9_{-2.2}^{+2.4}$	$B_s^0 \rightarrow f_1(1420)\bar{K}^0$	$-2.9_{-4.3}^{+3.7}$ $-67.9_{-5.8}^{+6.1}$ $73.4_{-6.0}^{+5.3}$
$B_d^0 \rightarrow f_1(1285)\eta$	$-80.9_{-15.4}^{+29.0}$ $-42.2_{-43.9}^{+48.2}$	$B_s^0 \rightarrow f_1(1285)\eta$	$1.0_{-0.9}^{+1.2}$ $0.9_{-1.6}^{+1.4}$ ~ 100
$B_d^0 \rightarrow f_1(1420)\eta$	$-93.6_{-9.2}^{+20.8}$ $-13.3_{-48.0}^{+51.8}$	$B_s^0 \rightarrow f_1(1420)\eta$	$-1.4_{-0.5}^{+0.4}$ $0.3_{-1.2}^{+0.9}$ ~ 100
$B_d^0 \rightarrow f_1(1285)\eta'$	$-47.7_{-25.5}^{+31.5}$ $-86.3_{-13.0}^{+20.1}$	$B_s^0 \rightarrow f_1(1285)\eta'$	$-2.5_{-0.9}^{+0.9}$ $-1.2_{-1.3}^{+1.4}$ ~ 100
$B_d^0 \rightarrow f_1(1420)\eta'$	$29.0_{-24.6}^{+24.1}$ $-44.2_{-16.5}^{+17.6}$	$B_s^0 \rightarrow f_1(1420)\eta'$	$1.5_{-0.8}^{+0.7}$ $0.5_{-1.0}^{+1.0}$ ~ 100

the time t_{CP} . The direct and mixing-induced CP -violating asymmetries $A_{CP}^{\text{dir}}(\mathcal{C}_f)$ and $A_{CP}^{\text{mix}}(\mathcal{S}_f)$ can be written as

$$A_{CP}^{\text{dir}} = \mathcal{C}_f = \frac{|\lambda_{CP}|^2 - 1}{1 + |\lambda_{CP}|^2}, \quad A_{CP}^{\text{mix}} = \mathcal{S}_f = \frac{2\text{Im}(\lambda_{CP})}{1 + |\lambda_{CP}|^2}, \quad (82)$$

with the CP -violating parameter λ_{CP}

$$\lambda_{CP} \equiv \eta_f \frac{V_{tb}^* V_{td(s)}}{V_{tb} V_{td(s)}^*} \cdot \frac{\langle f_{CP} | H_{eff} | \bar{B}_{d(s)}^0 \rangle}{\langle f_{CP} | H_{eff} | B_{d(s)}^0 \rangle}, \quad (83)$$

where η_f is the CP -eigenvalue of the final states. Moreover, for B_s^0 meson decays, a non-zero ratio $(\Delta\Gamma/\Gamma)_{B_s^0}$ is expected in the SM [53, 54]. For $B_s^0 \rightarrow f_1(\pi^0, \bar{K}^0, \eta, \eta')$ decays, the third term $A_{\Delta\Gamma_s}$ related to the presence of a non-negligible $\Delta\Gamma_s$ to describe the CP violation can be defined as follows [54]:

$$A_{\Delta\Gamma_s} = \frac{2\text{Re}(\lambda_{CP})}{1 + |\lambda_{CP}|^2}. \quad (84)$$

The three quantities describing the CP violation in B_s^0 meson decays shown in Eqs. (82) and (84) satisfy the following relation,

$$|A_{CP}^{\text{dir}}|^2 + |A_{CP}^{\text{mix}}|^2 + |A_{\Delta\Gamma_s}|^2 = 1. \quad (85)$$

Then, with the decay amplitudes for $B_{d(s)}^0 \rightarrow f_1(\pi^0, K_S^0(\bar{K}_S^0), \eta, \eta')$ decays as shown in the last section and the definitions in the above Eqs. (82) -(84), the direct and mixing-induced CP -violating asymmetries have been calculated in the pQCD approach within large theoretical errors and displayed in Table IV. Some remarks are in order:

- (1) As observed clearly from Table IV, almost all of the $b \rightarrow d$ transition processes have the large direct CP violations with still large uncertainties, while most of the $b \rightarrow s$ transition ones get the very small direct CP asymmetries except for $B_s^0 \rightarrow f_1\pi^0$ modes.
- (2) The relation of $A_{CP}^{\text{dir}}(B_d^0 \rightarrow f_1(1285)K_S^0) \sim 4 \times A_{CP}^{\text{dir}}(B_d^0 \rightarrow f_1(1420)K_S^0)$ can be found straightforwardly from Table IV. The underlying reason is with different contributions from tree diagrams because of the dominance of the f_{1s} (f_{1q}) component in $f_1(1420)$ [$f_1(1285)$] in the current mixing form. The same explanation can also be counted for the relation $A_{CP}^{\text{dir}}(B^+ \rightarrow f_1K^+) \gg A_{CP}^{\text{dir}}(B_d^0 \rightarrow f_1K_S^0)$ in magnitudes. Of course, as emphasized in the item on the discussions of the branching ratios of $B^+ \rightarrow f_1K^+$ and $B_d^0 \rightarrow f_1K_S^0$ decays, the latter modes are more like purely penguin-dominated channels.
- (3) It is interesting to note that those decays associated with very small direct CP violations but with very large CP -averaged branching ratios are almost purely penguin-dominated modes, whose tree pollution is so tiny that the numerical values of the decay rates remain unchanged when just the penguin contributions are taken into account. Actually, these mentioned decays, i.e., $B_d^0 \rightarrow f_1K_S^0$ and $B_s^0 \rightarrow f_1(\eta, \eta')$, are induced by the $b \rightarrow sq\bar{q}$ mediated transitions with $q = u, d, s$ at the quark level. For the latter modes, in principle, we can utilize the mixing-induced CP asymmetries to study the $B_s^0 - \bar{B}_s^0$ mixing phase ϕ_s . Unfortunately, however, these predictions in the pQCD approach suffer from significantly large theoretical errors arising from the much less constrained hadronic parameters. Therefore, this issue have to be left for future studies when the effective constraints are available from the experiments and/or nonperturbative techniques such as LQCD calculations. In the next subsection, we will analyze the $B_d^0 - \bar{B}_d^0$ mixing phase ϕ_d explicitly through the $B_d^0 \rightarrow f_1K_S^0$ modes.
- (4) The third CP -asymmetric observables $A_{\Delta\Gamma_s}$ for the B_s^0 meson decays are also listed in Table IV, in which we can find near 100% for most of the B_s^0 decay modes within large errors, apart from the $B_s^0 \rightarrow f_1(1420)\bar{K}^0$ channel around 70%. These interesting predictions in the pQCD approach and the resultant phenomenologies are expected to be examined by the highly precise measurements at the running LHCb and forthcoming Belle II experiments in the future.

C. Information on CKM weak phases α, β , and γ from $B \rightarrow f_1P$ decays

It is of great interest to note that the $B^+ \rightarrow f_1\pi^+$ decays are $b \rightarrow d(\Delta S = 0)$ transitions dominated by the tree diagrams, while the $B^+ \rightarrow f_1K^+$ decays are $b \rightarrow s(\Delta S = 1)$ ones determined by the penguin contributions. These unique properties exhibited in the $B^+ \rightarrow f_1(\pi^+, K^+)$ decays motivate us to further explore more useful information on the CKM weak phases α and γ by employing the careful investigations on the large CP -averaged branching ratios and the large direct CP asymmetries of $B^+ \rightarrow f_1(\pi^+, K^+)$ decays in the pQCD approach.

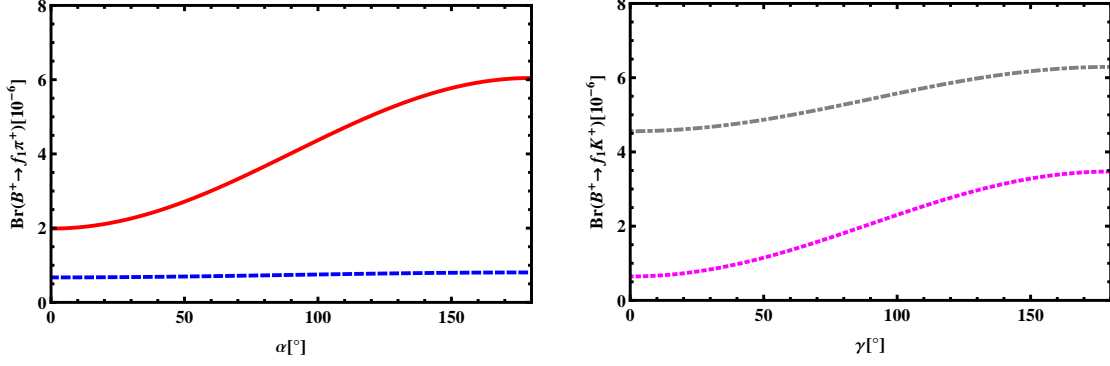


FIG. 3. (Color online) Dependence on the CKM weak phase $\alpha(\gamma)$ of central values of the CP -averaged branching ratios for $B^+ \rightarrow f_1 \pi^+ (K^+)$ decays in the pQCD approach. The red solid [blue dashed] line corresponds to the $B^+ \rightarrow f_1(1285)\pi^+$ [$f_1(1420)\pi^+$] decay and the magenta dotted [gray dot-dashed] one corresponds to the $B^+ \rightarrow f_1(1285)K^+$ [$f_1(1420)K^+$] mode, respectively.

We know that the decay amplitudes \mathcal{A}_f of $B^+ \rightarrow f_1(\pi^+, K^+)$ can be further written as the following forms,

$$\mathcal{A}_f(B^+ \rightarrow f_1 \pi^+) = \lambda_u^d T - \lambda_t^d P = \lambda_u^d T \{1 + r \exp[i(\alpha + \delta)]\}, \quad (86)$$

$$\mathcal{A}_f(B^+ \rightarrow f_1 K^+) = \lambda_u^s T' - \lambda_t^s P' = \lambda_u^s T' \{1 + r' \exp[i(\gamma' + \delta')]\}, \quad (87)$$

where $T(T')$ and $P(P')$ denote the tree and penguin decay amplitudes of $B^+ \rightarrow f_1 \pi^+ (K^+)$ decays, and $r(r')$ and $\delta(\delta')$ represent the ratios of penguin to tree contributions $\frac{|\lambda_t^d||P|}{|\lambda_u^d||T|}$ ($\frac{|\lambda_t^s||P'|}{|\lambda_u^s||T'|}$) and the relative strong phases between the corresponding tree and penguin diagrams. The weak phase α come from the identity $\alpha = 180^\circ - \beta - \gamma$ with the definitions $V_{td} = |V_{td}| \exp(-i\beta)$ and $V_{ub} = |V_{ub}| \exp(-i\gamma)$, and the γ' is defined as $\arg[-\frac{V_{tb}^* V_{ts}}{V_{ub}^* V_{us}}]$. Then the decay amplitudes $\bar{\mathcal{A}}_f$ of the charge conjugated modes $B^- \rightarrow f_1(\pi^-, K^-)$ can be easily written as

$$\bar{\mathcal{A}}_f(B^- \rightarrow f_1 \pi^-) = (\lambda_u^d)^* T - (\lambda_t^d)^* P = (\lambda_u^d)^* T \{1 + r \exp[i(-\alpha + \delta)]\}, \quad (88)$$

$$\bar{\mathcal{A}}_f(B^- \rightarrow f_1 K^-) = (\lambda_u^s)^* T' - (\lambda_t^s)^* P' = (\lambda_u^s)^* T' \{1 + r' \exp[i(-\gamma' + \delta')]\}. \quad (89)$$

Therefore, the CP -averaged branching ratios can be read as

$$Br(B^+ \rightarrow f_1 \pi^+) \equiv \frac{|\bar{\mathcal{A}}_f|_{f_1 \pi^-}^2 + |\mathcal{A}_f|_{f_1 \pi^+}^2}{2} = |\lambda_u^d T|^2 \{1 + 2r \cos \alpha \cos \delta + r^2\}, \quad (90)$$

$$Br(B^+ \rightarrow f_1 K^+) \equiv \frac{|\bar{\mathcal{A}}_f|_{f_1 K^-}^2 + |\mathcal{A}_f|_{f_1 K^+}^2}{2} = |\lambda_u^s T'|^2 \{1 + 2r' \cos \gamma \cos \delta' + r'^2\}, \quad (91)$$

in which $T^{(\prime)}$, $r^{(\prime)}$, and $\delta^{(\prime)}$ are all perturbatively calculated in the pQCD approach; also, $\lambda_u^{d,s}$ are determined from the experiments. Thus, Eqs. (90) and (91) can provide a possible way to determine the CKM angles α and γ potentially by measuring the branching ratios, respectively. In Fig. 3, we show the central values of the CP -averaged branching ratios for $B^+ \rightarrow f_1(1285)\pi^+$ (red solid line) and $B^+ \rightarrow f_1(1420)\pi^+$ (blue dashed line) [$B^+ \rightarrow f_1(1285)K^+$ (magenta dotted line) and $B^+ \rightarrow f_1(1420)K^+$ (gray dot-dashed line)] decays as a function of the CKM weak phase $\alpha[\gamma]$ in the pQCD approach. One can easily see the strong (weak) dependence on α for $B^+ \rightarrow f_1(1285)\pi^+$ [$f_1(1420)\pi^+$] decay and the moderate dependence on γ for $B^+ \rightarrow f_1 K^+$ decays in the pQCD approach from Fig. 3. One can also directly observe from Fig. 3 that the central values of the branching ratios for the considered decays in the pQCD approach correspond to the central values of α and γ as around 89° and 70° , respectively, which are very consistent with the constraints from various experiments [3].

More information on the CKM angles α and γ can also be hinted from the large direct CP asymmetries of $B^+ \rightarrow f_1 \pi^+ (K^+)$ decays in the pQCD approach. With Eqs. (86)~(89), the direct CP -violating asymmetry Eq. (78) for $B^+ \rightarrow f_1 \pi^+ (K^+)$ can be described as the function of $\alpha(\gamma)$,

$$A_{CP}^{\text{dir}}(B^+ \rightarrow f_1 \pi^+) = \frac{2r \sin \alpha \sin \delta}{1 + 2r \cos \alpha \cos \delta + r^2}, \quad (92)$$

$$A_{CP}^{\text{dir}}(B^+ \rightarrow f_1 K^+) = -\frac{2r' \sin \gamma \sin \delta'}{1 + 2r' \cos \gamma \cos \delta' + r'^2}. \quad (93)$$

Again, as aforementioned, the ratios $r^{(\prime)}$ and the relative strong phases $\delta^{(\prime)}$ can be explicitly calculated in the pQCD approach. Undoubtedly, the former Eq. (92) is a function of $\sin \alpha$ and $\cos \alpha$, and the latter Eq. (93) is a function of $\sin \gamma$ and $\cos \gamma$. In

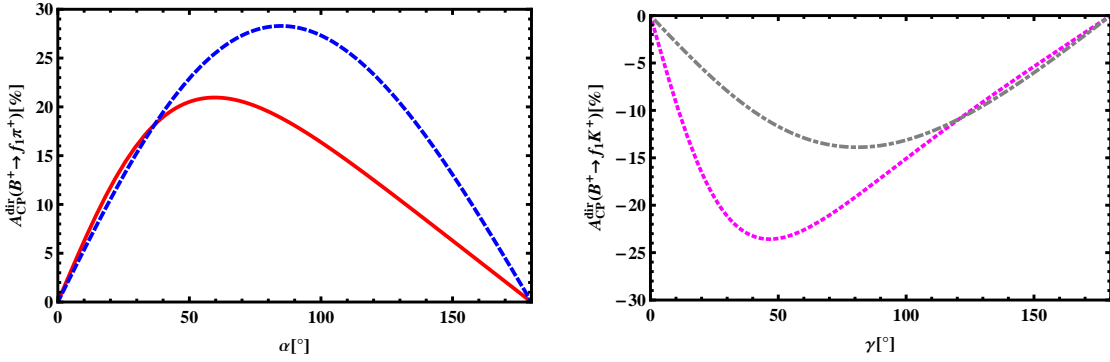


FIG. 4. (Color online) Dependence on the CKM weak phase $\alpha(\gamma)$ of central values of the direct CP -violating asymmetries for $B^+ \rightarrow f_1 \pi^+ (K^+)$ decays in the pQCD approach. The red solid [blue dashed] line corresponds to the $B^+ \rightarrow f_1(1285) \pi^+ [f_1(1285) \pi^+]$ decay and the magenta dotted[gray dot-dashed] one corresponds to the $B^+ \rightarrow f_1(1285) K^+ [f_1(1420) K^+]$ decay, respectively.

particular, if one mode like $B^+ \rightarrow f_1(1420) \pi^+$ is almost completely tree dominated, i.e., $r \ll 1$, then Eq. (92) can be further written approximately as

$$A_{CP}^{\text{dir}}(B^+ \rightarrow f_1(1420) \pi^+) \sim 2r \sin \alpha \sin \delta. \quad (94)$$

Analogously, if one mode like $B^+ \rightarrow f_1(1420) K^+$ is nearly pure penguin contributions, i.e., $r' \gg 1$, then Eq. (93) can be further described approximately as

$$A_{CP}^{\text{dir}}(B^+ \rightarrow f_1 K^+) \sim -\frac{2}{r'} \sin \gamma \sin \delta'. \quad (95)$$

Thus, the large direct CP -violating asymmetries driven by these two equations, i.e., Eqs. (94) and (95), will give rise to the effective constraints more easily on the CKM phases α and γ from the experimental data with high precision. Certainly, based on Eqs. (94) and (95), the large strong phases δ and δ' required by the large direct CP asymmetries can also be deduced naturally.

The central values of the large direct CP violations for the $B^+ \rightarrow f_1(1285) \pi^+$ (red solid line) and $B^+ \rightarrow f_1(1420) \pi^+$ (blue dashed line) [$B^+ \rightarrow f_1(1285) K^+$ (magenta dashed line) and $B^+ \rightarrow f_1(1420) K^+$ (gray dot-dashed line)] decays as a function of the CKM weak phase $\alpha[\gamma]$ in the pQCD approach have also been shown in Fig. 4. One can find straightforwardly from Fig. 4 that $A_{CP}^{\text{dir}}(B^+ \rightarrow f_1 \pi^+)$ are large and positive, while $A_{CP}^{\text{dir}}(B^+ \rightarrow f_1 K^+)$ are large and negative, which are expected to be tested by the experiments in the near future.

It is important to note that the mixing-induced CP -violating asymmetries of the $B_d^0 \rightarrow f_1 K_S^0$ decays are with the very small uncertainties as seen clearly in Table IV, which, as the alternative channels, are expected to have the supplementary power in reducing the errors of the CKM weak phase β . We can write the expression of the CP -violating parameter $\lambda_{CP}(f_1 K_S^0)$ in an explicit form,

$$\lambda_{CP}(f_1 K_S^0) = -\exp(-2i\beta) \frac{|\lambda_u^s| T_{f_1 K_S^0} \exp(-i\gamma) - |\lambda_t^s| P_{f_1 K_S^0}}{|\lambda_u^s| T_{f_1 K_S^0} \exp(i\gamma) - |\lambda_t^s| P_{f_1 K_S^0}}. \quad (96)$$

Here, $|\lambda_u^s| \sim 0.02 \cdot |\lambda_t^s|$ and $T_{f_1 K_S^0}$ is the decay amplitude arising from the color-suppressed tree diagrams, which will consequently result in the negligible tree pollution relative to the much larger penguin contributions in the $B_d^0 \rightarrow f_1 K_S^0$ decays, and then $\lambda_{CP}(f_1 K_S^0) \approx -\exp(-2i\beta)$, i.e., $A_{CP}^{\text{mix}} = \mathcal{S}_f \sim \sin(2\beta_{\text{eff}})$. In principle, the results should be identical to those measuring the $\mathcal{S}_f = -\eta_f \sin 2\beta$ from the tree dominated $b \rightarrow c\bar{c}s$ transitions, such as the theoretically cleanest $B_d^0 \rightarrow J/\psi K_{S,L}^0$. However, the $b \rightarrow s\bar{q}q$ decays are potentially contaminated by the indeed existing tree pollution. Then the deviation between $\mathcal{S}_{\text{penguin}}$ and $\mathcal{S}_{\text{c}\bar{c}s}$ can be defined as $\Delta\mathcal{S} \equiv \mathcal{S}_{\text{penguin}} - \mathcal{S}_{\text{c}\bar{c}s}$, which will be helpful to justify the discrepancies as promising new physics signals. Up to now, the world average value of the $\mathcal{S}_{\text{c}\bar{c}s}$ at the experimental aspect is [3]

$$\sin 2\beta = 0.682 \pm 0.019. \quad (97)$$

Then our pQCD predictions of $\sin 2\beta_{\text{eff}}$ for the $B_d^0 \rightarrow f_1 K_S^0$ decays deviate to the $\sin 2\beta$ as

$$\Delta\mathcal{S}_{f_1(1285)K_S^0} \approx 0.018_{-0.035}^{+0.036}, \quad \Delta\mathcal{S}_{f_1(1420)K_S^0} \approx 0.017_{-0.029}^{+0.031}, \quad (98)$$

which are well below the bound, at most $\mathcal{O}(0.1)$ [55], and can be confronted with stringent tests by the future experiments.

IV. CONCLUSIONS AND SUMMARY

In this work, we have studied the CP -averaged branching ratios and the CP -violating asymmetries of 20 charmless hadronic $B \rightarrow f_1 P$ decays within the framework of the pQCD approach. We explicitly evaluated the nonfactorizable spectator and annihilation types of diagrams, except for the traditional factorizable emission ones. Based on the quark-flavor mixing of the $f_1(1285) - f_1(1420)$ system with the angle $\phi_{f_1} \sim 24^\circ$ extracted first from the B meson decays, we calculated the numerical results for the considered physical observables and made the phenomenological discussions, correspondingly. The main conclusions of the present paper are as follows:

- (1) For the four charged $B^+ \rightarrow f_1 \pi^+ (\Delta S = 0)$ and $f_1 K^+ (\Delta S = 1)$ decays, the large CP -averaged branching ratios [$\mathcal{O}(10^{-6})$] together with the large direct CP asymmetries predicted in the pQCD approach are believed to be clearly measurable at the running LHC and forthcoming Belle II experiments in the near future. Furthermore, it is expected that they could provide supplementary constraints on the CKM weak phase $\alpha (\gamma)$ because of the correspondingly tree-dominant (penguin-dominant) contributions to the former(latter) decays. Of course, inferred from the numerical results for the large decay rates theoretically and the preliminary upper limits for the branching ratios of $B^+ \rightarrow f_1 K^+$ modes experimentally, the region of angle ϕ_{f_1} can be deduced as $\phi_{f_1} \in [20^\circ, 27^\circ]$ by combining with the earlier phenomenological analysis, experimental measurements and updated LQCD calculations, which provide more evidence for the dominance of f_{1q} [f_{1s}] in $f_1(1285)$ [$f_1(1420)$].
- (2) Based on the CP -averaged branching ratios of $B \rightarrow f_1(\pi, K)$ decays calculated in the pQCD approach, the destructive or constructive interferences between $f_{1q}(\pi, K)$ and $f_{1s}(\pi, K)$ states can be clearly observed and are expected to be confronted with the future experiments. Also, besides the effects from the $f_{1q} - f_{1s}$ mixing, the $B_{d/s}^0 \rightarrow f_1(\eta, \eta')$ modes embrace another set of interferences from $\eta_q - \eta_s$ mixing for $\eta - \eta'$ system simultaneously, which makes more complicated interactions among the four $B_{d(s)}^0 \rightarrow f_{1q}\eta_q, f_{1q}\eta_s, f_{1s}\eta_q$, and $f_{1s}\eta_s$ states.
- (3) For the eight neutral $B_{d,s}^0 \rightarrow f_1(\pi^0, \eta, \eta', \bar{K}^0)$ decays, they are mediated by the $b \rightarrow d$ transitions and dominated by the penguin amplitudes just with small color-suppressed tree contributions, which then lead to the small CP -averaged branching ratios in the order of $10^{-8} \sim 10^{-7}$ that cannot be measured by the experiments in a short period.
- (4) The remaining eight neutral $B_{s,d}^0 \rightarrow (\pi^0, \eta, \eta', K_S^0)$ modes decay through $b \rightarrow s$ transitions and have large CP -averaged branching ratios in the order of $10^{-6} \sim 10^{-5}$, except for $B_s^0 \rightarrow f_1 \pi^0$ decays. The channels with large decay rates are all contributed by the nearly pure penguin amplitudes with tiny and safely negligible tree pollution, which can be easily accessed at the ongoing LHCb experiments in the near future.
- (5) In principle, $B_d^0 \rightarrow f_1 K_S^0$ and $B_s^0 \rightarrow f_1(\eta, \eta')$ modes can serve as the alternative channels to provide more information on the $B_d^0 - \bar{B}_d^0$ and $B_s^0 - \bar{B}_s^0$ mixing phases from the mixing-induced CP asymmetries \mathcal{S}_f , respectively. However, the latter B_s^0 decays suffer from large theoretical uncertainties that consequently result in the less effective constraints on the mixing phase ϕ_s . Fortunately, the former B_d^0 ones induced by the $b \rightarrow sq\bar{q}$ decays have large mixing-induced CP -violating asymmetries but with very small errors. The resultant deviations of $\Delta\mathcal{S}$ for $B_d^0 \rightarrow f_1(1285)K_S^0$ and $f_1(1420)K_S^0$ are around 0.02, which will be stringently examined by the experiments with high precision.
- (6) The weak annihilation contributions to these 20 $B \rightarrow f_1 P$ decays have been examined in the pQCD approach. The numerical results show that the sizable effects from annihilation diagrams play important roles in the $B_{u,d} \rightarrow f_1(1420)K$, $B_d^0 \rightarrow f_1 \eta', f_1(1420)(\pi, \eta)$, and $B_s^0 \rightarrow f_1(1285)\bar{K}^0, f_1(1420)\eta'$ decays. The remaining channels do not depend sensitively on the weak annihilation contributions. The reliability of the evaluations of the weak annihilation diagrams made in the pQCD approach should be strictly examined by the future experiments, which can help to distinguish the different viewpoints on calculating the annihilation diagrams proposed by the pQCD approach and soft-collinear effective theory, and then to further understand the annihilation decay mechanism in the heavy b -flavored meson decays.
- (7) Admittedly, our pQCD results suffer from large theoretical errors induced by the less constrained hadronic parameters, in particular, from the axial-vector f_1 mesons' wave function presently. Meanwhile, only the short-distance contributions at leading order without considering the final state interactions have been taken into account. However, the channels such as $B^+ \rightarrow f_1(\pi^+, K^+)$, $B_d^0 \rightarrow f_1 K_S^0$, and $B_s^0 \rightarrow f_1(\eta, \eta')$ with large branching ratios are easily accessible in the near future measurements with precision at LHCb and/or Belle II experiments, which are expected in turn to provide useful information on improving the input quantities; on the other hand, they can help to understand the mixing angle ϕ_{f_1} and the nature of both f_1 mesons better and to identify the reliability of the perturbative evaluations of QCD factorization and the pQCD approach in these decays involving axial-vector mesons.

ACKNOWLEDGMENTS

X.L. thanks the Institute of Physics at Academia Sinica Taiwan for the warm hospitality during his visit, where part of this work was finalized. This work is supported by the National Natural Science Foundation of China under Grants No. 11205072, No. 11235005, and No. 11047014, and by a project funded by the Priority Academic Program Development of Jiangsu Higher Education Institutions (PAPD), by the Research Fund of Jiangsu Normal University under Grant No. 11XLR38, and by the Foundation of Yantai University under Grant No. WL07052.

Appendix A: Hadrons' distribution amplitudes

For the B meson, the distribution amplitude in the impact b space has been proposed as [10, 11]

$$\phi_B(x, b) = N_B x^2 (1-x)^2 \exp \left[-\frac{1}{2} \left(\frac{x m_B}{\omega_b} \right)^2 - \frac{\omega_b^2 b^2}{2} \right], \quad (\text{A1})$$

where the normalization factor N_B is related to the decay constant f_B through Eq. (14). The shape parameter ω_b has been fixed at $\omega_b = 0.40$ GeV by using the rich experimental data on the $B_{u,d}$ mesons with $f_{B_{u,d}} = 0.19$ GeV based on lots of calculations of form factors [34] and other well-known decay modes of $B_{u,d}$ mesons [10, 11] in the pQCD approach in recent years. Because the s quark is heavier than the u or d quark, the momentum fraction of the s quark should be a little larger than that of the u or d quark in the $B_{u,d}$ mesons. Therefore, by considering a small SU(3) symmetry breaking, we adopt the shape parameter $\omega_{bs} = 0.50$ GeV [24] with $f_{B_s} = 0.23$ GeV for the B_s meson, and the corresponding normalization constant is $N_{B_s} = 63.67$. In order to analyze the uncertainties of theoretical predictions induced by the inputs, we can vary the shape parameters ω_b and ω_{bs} by 10%, i.e., $\omega_b = 0.40 \pm 0.04$ GeV and $\omega_{bs} = 0.50 \pm 0.05$ GeV, respectively.

The twist-2 pseudoscalar meson distribution amplitude $\phi_{\pi,K}^A$ and the twist-3 ones $\phi_{\pi,K}^P$ and $\phi_{\pi,K}^T$ have been parametrized as [35, 36, 56]

$$\phi_{\pi,K}^A(x) = \frac{f_{\pi,K}}{2\sqrt{2N_c}} 6x(1-x) \left[1 + a_1^{\pi,K} C_1^{3/2}(2x-1) + a_2^{\pi,K} C_2^{3/2}(2x-1) + a_4^{\pi,K} C_4^{3/2}(2x-1) \right], \quad (\text{A2})$$

$$\begin{aligned} \phi_{\pi,K}^P(x) = \frac{f_{\pi,K}}{2\sqrt{2N_c}} \left[1 + \left(30\eta_3 - \frac{5}{2}\rho_{\pi,K}^2 \right) C_2^{1/2}(2x-1) \right. \\ \left. - 3 \left\{ \eta_3\omega_3 + \frac{9}{20}\rho_{\pi,K}^2(1 + 6a_2^{\pi,K}) \right\} C_4^{1/2}(2x-1) \right], \end{aligned} \quad (\text{A3})$$

$$\phi_{\pi,K}^T(x) = \frac{f_{\pi,K}}{2\sqrt{2N_c}} (1-2x) \left[1 + 6 \left(5\eta_3 - \frac{1}{2}\eta_3\omega_3 - \frac{7}{20}\rho_{\pi,K}^2 - \frac{3}{5}\rho_{\pi,K}^2 a_2^{\pi,K} \right) (1-10x+10x^2) \right], \quad (\text{A4})$$

with the Gegenbauer moments $a_1^\pi = 0, a_1^K = 0.17 \pm 0.17, a_2^{\pi,K} = 0.115 \pm 0.115, a_4^{\pi,K} = -0.015$; the mass ratio $\rho_{\pi,K} = m_{\pi,K}/m_0^{\pi,K}$ and $\rho_{\eta_q(s)} = 2m_{q(s)}/m_{qq(ss)}$; and the Gegenbauer polynomials $C_n^\nu(t)$,

$$\begin{aligned} C_2^{1/2}(t) &= \frac{1}{2} (3t^2 - 1), \quad C_4^{1/2}(t) = \frac{1}{8} (3 - 30t^2 + 35t^4), \\ C_1^{3/2}(t) &= 3t, \quad C_2^{3/2}(t) = \frac{3}{2} (5t^2 - 1), \quad C_4^{3/2}(t) = \frac{15}{8} (1 - 14t^2 + 21t^4). \end{aligned} \quad (\text{A5})$$

In the above distribution amplitudes for the kaon, the momentum fraction x is carried by the s quark. For both the pion and kaon, we choose $\eta_3 = 0.015$ and $\omega_3 = -3$ [35, 36].

For the axial-vector states $f_{1q(s)}$, its leading twist light-cone distribution amplitude in the longitudinal polarization can generally be expanded as the Gegenbauer polynomials [37]:

$$\phi_{f_{1q(s)}}(x) = \frac{f_{f_{1q(s)}}}{2\sqrt{2N_c}} 6x(1-x) \left[1 + a_{2f_{1q(s)}}^\parallel \frac{3}{2} (5(2x-1)^2 - 1) \right]. \quad (\text{A6})$$

For twist-3 light-cone distribution amplitudes, we use the following form [38]:

$$\phi_{f_{1q(s)}}^s(x) = \frac{f_{f_{1q(s)}}}{4\sqrt{2N_c}} \frac{d}{dx} \left[6x(1-x) (a_{1f_{1q(s)}}^\perp (2x-1)) \right], \quad (\text{A7})$$

$$\phi_{f_{1q(s)}}^t(x) = \frac{f_{f_{1q(s)}}}{2\sqrt{2N_c}} \left[\frac{3}{2} a_{1f_{1q(s)}}^\perp (2x-1) (3(2x-1)^2 - 1) \right], \quad (\text{A8})$$

where the Gegenbauer moments are quoted from Ref. [37] as

$$f_{1q} \text{ state : } \quad a_2^{\parallel} = -0.02 \pm 0.02, \quad a_1^{\perp} = -1.04 \pm 0.34; \quad (\text{A9})$$

and

$$f_{1s} \text{ state : } \quad a_2^{\parallel} = -0.04 \pm 0.03; \quad a_1^{\perp} = -1.06 \pm 0.36, \quad (\text{A10})$$

where the values are taken at $\mu = 1 \text{ GeV}$.

-
- [1] T. Feldmann, arXiv:1408.0300 [hep-ph]; W. Wang, R. H. Li and C. D. Lü, Phys. Rev. D **78**, 074009 (2008).
 - [2] G. Calderon, J. H. Munoz and C. E. Vera, Phys. Rev. D **76**, 094019 (2007).
 - [3] K. A. Olive *et al.* [Particle Data Group Collaboration], Chin. Phys. C **38**, 090001 (2014).
 - [4] R. Aaij *et al.* [LHCb Collaboration], Phys. Rev. Lett. **112**, 091802 (2014).
 - [5] F. E. Close and A. Kirk, Z. Phys. C **76**, 469 (1997).
 - [6] D. M. Li, H. Yu and Q. X. Shen, Chin. Phys. Lett. **17**, 558 (2000).
 - [7] X. Liu and Z. J. Xiao, Phys. Rev. D **89**, 097503 (2014).
 - [8] H. Y. Cheng, Phys. Lett. B **707**, 116 (2012).
 - [9] X. Liu and Z. J. Xiao, Phys. Rev. D **81**, 074017 (2010); Z. J. Xiao and X. Liu, Chin. Sci. Bull. **59**, 3748 (2014).
 - [10] Y. Y. Keum, H.-n. Li and A. I. Sanda, Phys. Lett. B **504**, 6 (2001); Phys. Rev. D **63**, 054008 (2001).
 - [11] C. D. Lü, K. Ukai and M. Z. Yang, Phys. Rev. D **63**, 074009 (2001).
 - [12] H.-n. Li, Prog. Part. Nucl. Phys. **51**, 85 (2003).
 - [13] J. P. Burke [BaBar Collaboration], J. Phys. Conf. Ser. **110**, 052005 (2008).
 - [14] H. Y. Cheng and K. C. Yang, Phys. Rev. D **76**, 114020 (2007).
 - [15] G. Buchalla, A. J. Buras and M. E. Lautenbacher, Rev. Mod. Phys. **68**, 1125 (1996).
 - [16] H. n. Li, Y. L. Shen, Y. M. Wang and H. Zou, Phys. Rev. D **83**, 054029 (2011); H. n. Li, Y. L. Shen and Y. M. Wang, Phys. Rev. D **85**, 074004 (2012); J. High Energy Phys. **02**, 008 (2013); H. C. Hu and H. n. Li, Phys. Lett. B **718**, 1351 (2013).
 - [17] S. Cheng, Y. Y. Fan and Z. J. Xiao, Phys. Rev. D **89**, 054015 (2014); S. Cheng, Y. Y. Fan, X. Yu, C. D. L and Z. J. Xiao, Phys. Rev. D **89**, 094004 (2014); S. Cheng and Z. J. Xiao, Phys. Rev. D **90**, 076001 (2014); arXiv:1409.5947 [hep-ph].
 - [18] G. Zhu, Phys. Lett. B **702**, 408 (2011); K. Wang and G. Zhu, Phys. Rev. D **88**, 014043 (2013).
 - [19] Q. Chang, J. Sun, Y. Yang and X. Li, arXiv:1409.1322 [hep-ph]; Q. Chang, J. Sun, Y. Yang and X. Li, arXiv:1409.2995 [hep-ph].
 - [20] J. Chay, H.-n. Li and S. Mishima, Phys. Rev. D **78**, 034037 (2008).
 - [21] C. M. Arnesen, Z. Ligeti, I. Z. Rothstein and I. W. Stewart, Phys. Rev. D **77**, 054006 (2008).
 - [22] C. D. Lu and K. Ukai, Eur. Phys. J. C **28**, 305 (2003).
 - [23] Y. Li, C. D. Lu, Z. J. Xiao and X. Q. Yu, Phys. Rev. D **70**, 034009 (2004).
 - [24] A. Ali, G. Kramer, Y. Li, C. D. Lu, Y. L. Shen, W. Wang and Y. M. Wang, Phys. Rev. D **76**, 074018 (2007).
 - [25] Z. J. Xiao, W. F. Wang and Y. Y. Fan, Phys. Rev. D **85**, 094003 (2012).
 - [26] B. H. Hong and C. D. Lu, Sci. China G **49**, 357 (2006); H.-n. Li and S. Mishima, Phys. Rev. D **71**, 054025 (2005); H.-n. Li, Phys. Lett. B **622**, 63 (2005).
 - [27] T. Aaltonen *et al.* [CDF Collaboration], Phys. Rev. Lett. **108** (2012) 211803.
 - [28] F. Ruffini, FERMILAB-THESIS-2013-02.
 - [29] R. Aaij *et al.* [LHCb Collaboration], J. High Energy Phys. **10**, 037 (2012).
 - [30] H.-n. Li, Phys. Rev. D **66**, 094010 (2002).
 - [31] H.-n. Li and K. Ukai, Phys. Lett. B **555**, 197 (2003).
 - [32] J. Botts and G. F. Sterman, Nucl. Phys. B **325**, 62 (1989).
 - [33] H.-n. Li and G. F. Sterman, Nucl. Phys. B **381**, 129 (1992).
 - [34] C. D. Lu and M. Z. Yang, Eur. Phys. J. C **28**, 515 (2003).
 - [35] V. L. Chernyak and A. R. Zhitnitsky, Phys. Rept. **112**, 173 (1984); A. R. Zhitnitsky, I. R. Zhitnitsky and V. L. Chernyak, Sov. J. Nucl. Phys. **41**, 284 (1985) [Yad. Fiz. **41**, 445 (1985)]; V. M. Braun and I. E. Filyanov, Z. Phys. C **44**, 157 (1989) [Sov. J. Nucl. Phys. **50**, 511 (1989)] [Yad. Fiz. **50**, 818 (1989)]; V. M. Braun and I. E. Filyanov, Z. Phys. C **48**, 239 (1990) [Sov. J. Nucl. Phys. **52**, 126 (1990)] [Yad. Fiz. **52**, 199 (1990)].
 - [36] P. Ball, J. High Energy Phys. **09**, 005 (1998); P. Ball, J. High Energy Phys. **01**, 010 (1999).
 - [37] K. C. Yang, Nucl. Phys. B **776**, 187 (2007).
 - [38] R. H. Li, C. D. Lu and W. Wang, Phys. Rev. D **79**, 034014 (2009).
 - [39] X. Liu, H. s. Wang, Z. j. Xiao, L. Guo and C. D. Lu, Phys. Rev. D **73**, 074002 (2006).
 - [40] T. Feldmann, P. Kroll and B. Stech, Phys. Rev. D **58**, 114006 (1998).
 - [41] R. Escribano and J. M. Frere, J. High Energy Phys. **06**, 029 (2005); J. Schechter, A. Subbaraman and H. Weigel, Phys. Rev. D **48**, 339 (1993).
 - [42] C. Di Donato, G. Ricciardi and I. Bigi, Phys. Rev. D **85**, 013016 (2012).
 - [43] H. s. Wang, X. Liu, Z. j. Xiao, L. b. Guo and C. D. Lu, Nucl. Phys. B **738**, 243 (2006); Z. j. Xiao, D. q. Guo and X. f. Chen, Phys. Rev. D **75**, 014018 (2007); Z. j. Xiao, X. Liu and H. s. Wang, Phys. Rev. D **75**, 034017 (2007); D. Q. Guo, X. F. Chen and Z. J. Xiao, Phys. Rev.

- D **75**, 054033 (2007); Z. J. Xiao, Z. Q. Zhang, X. Liu and L. B. Guo, Phys. Rev. D **78**, 114001 (2008); X. Liu, H. n. Li and Z. J. Xiao, Phys. Rev. D **86**, 011501 (2012); Y. Y. Fan, W. F. Wang, S. Cheng and Z. J. Xiao, Phys. Rev. D **87**, 094003 (2013).
- [44] Y. Y. Charng, T. Kurimoto and H. n. Li, Phys. Rev. D **74**, 074024 (2006) [Erratum-ibid. D **78**, 059901 (2008)].
- [45] R. Escribano and J. Nadal, J. High Energy Phys. **05**, 006 (2007).
- [46] K. C. Yang, Phys. Rev. D **84**, 034035 (2011).
- [47] H. Y. Cheng, *Proc. Sci.*, Hadron2013, 090 (2014).
- [48] R. C. Verma, J. Phys. G **39**, 025005 (2012).
- [49] G. Gidal, J. Boyer, F. Butler, D. Cords, G. S. Abrams, D. Amidei, A. R. Baden and T. Barklow *et al.*, Phys. Rev. Lett. **59**, 2012 (1987).
- [50] J. J. Dudek, R. G. Edwards, P. Guo and C. E. Thomas, Phys. Rev. D **88**, 094505 (2013)
- [51] J. Beringer *et al.* [Particle Data Group Collaboration], Phys. Rev. D **86**, 010001 (2012).
- [52] J. F. Donoghue, B. R. Holstein and Y. C. R. Lin, Phys. Rev. Lett. **55**, 2766 (1985) [Erratum-ibid. **61**, 1527 (1988)].
- [53] M. Beneke, G. Buchalla, C. Greub, A. Lenz and U. Nierste, Phys. Lett. B **459**, 631 (1999).
- [54] L. Fernandez, CERN-THESIS-2006-042.
- [55] D. London and A. Soni, Phys. Lett. B **407**, 61 (1997).
- [56] V. M. Braun and A. Lenz, Phys. Rev. D **70**, 074020 (2004); P. Ball and A. N. Talbot, J. High Energy Phys. **06**, 063 (2005); P. Ball and R. Zwicky, Phys. Lett. B **633**, 289 (2006); A. Khodjamirian, T. Mannel and M. Melcher, Phys. Rev. D **70**, 094002 (2004).